SANDIA REPORT

SAND2014-17935
Unlimited Release
Printed September 2014

Room temperature creep in metals and alloys

Lisa A. Deibler

Prepared by
Sandia National Laboratories
Albuquerque, New Mexico 87185 and Livermore, California 94550

Sandia National Laboratories is a multi-program laboratory managed and operated by Sandia Corporation, a wholly owned subsidiary of Lockheed Martin Corporation, for the U.S. Department of Energy's National Nuclear Security Administration under contract DE-AC04-94AL85000.

Approved for public release; further dissemination unlimited.

Sandia National Laboratories

Issued by Sandia National Laboratories, operated for the United States Department of Energy by Sandia Corporation.

NOTICE: This report was prepared as an account of work sponsored by an agency of the United States Government. Neither the United States Government, nor any agency thereof, nor any of their employees, nor any of their contractors, subcontractors, or their employees, make any warranty, express or implied, or assume any legal liability or responsibility for the accuracy, completeness, or usefulness of any information, apparatus, product, or process disclosed, or represent that its use would not infringe privately owned rights. Reference herein to any specific commercial product, process, or service by trade name, trademark, manufacturer, or otherwise, does not necessarily constitute or imply its endorsement, recommendation, or favoring by the United States Government, any agency thereof, or any of their contractors or subcontractors. The views and opinions expressed herein do not necessarily state or reflect those of the United States Government, any agency thereof, or any of their contractors.

Printed in the United States of America. This report has been reproduced directly from the best available copy.

Available to DOE and DOE contractors from
U.S. Department of Energy
Office of Scientific and Technical Information
P.O. Box 62
Oak Ridge, TN 37831

Telephone: (865) 576-8401
Facsimile: (865) 576-5728
E-Mail: reports@adonis.osti.gov
Online ordering: http://www.osti.gov/bridge

Available to the public from
U.S. Department of Commerce
National Technical Information Service
5285 Port Royal Rd
Springfield, VA 22161

Telephone: (800) 553-6847
Facsimile: (703) 605-6900
E-Mail: orders@ntis.fedworld.gov
Online ordering: http://www.ntis.gov/help/ordermethods.asp?loc=7-4-0#online

SAND2014-17935
Unlimited Release
Printed September 2014

Room temperature creep in metals and alloys

Lisa A. Deibler

Materials Characterization and Performance
Sandia National Laboratories
Mail Stop 0886
PO Box 5800
Albuquerque, NM 87185-0886

Abstract

Time dependent deformation in the form of creep and stress relaxation is not often considered a factor when designing structural alloy parts for use at room temperature. However, creep and stress relaxation do occur at room temperature (0.09-0.21 T_m for alloys in this report) in structural alloys. This report will summarize the available literature on room temperature creep, present creep data collected on various structural alloys, and finally compare the acquired data to equations used in the literature to model creep behavior. Based on evidence from the literature and fitting of various equations, the mechanism which causes room temperature creep is found to include dislocation generation as well as exhaustion.

Acknowledgment

Thanks to Tom Crenshaw for assistance with creep experiments and Brad Boyce and Joe Puskar for helpful discussions on room temperature creep.

Contents

Introduction . . . 7
Literature review . . . 8
  Time dependent deformation influencing designs . . . 8
  Hydrogen effects on room temperature creep . . . 9
  Constant dislocation density . . . 9
  Source activation of dislocations . . . 12
Experimental procedure . . . 18
Results . . . 20
Discussion . . . 29
  Observations about the creep data presented in the results section . . . 29
  Fitting data from the results section to models from literature . . . 32
Conclusion . . . 40
References . . . 41

Figures

1 Long term dead weight tests: a) before loading, b) within one minute of loading, c)24 hours after loading, d) 3 months after loading . . . 19
2 Total strain caused by a multiple load creep test on 304L wire. . . . 20
3 Pure Cu wire creep curves at various loads . . . 21
4 304L wire creep curves at various loads . . . 22
5 Creep curves on a wrought 304L tensile sample . . . 22
6 Creep curves from a cast 304L tensile sample . . . 23
7 Creep curves from a 2024 Al sample . . . 23
8 Creep curves from a pure Cu sample. . . . 24
9 Creep curves from a Ta-10W sample . . . 24
10 Creep curves from a pure Ta sample . . . 25
11 Creep curves from a 17-4 sample . . . 25
12 Creep curves from a 13-8 sample . . . 26
13 Creep curves from a Nitronic 50 transverse sample . . . 27
14 Total strain (including instantaneous strain) from long-term creep tests. Data is well-behaved up until about 3 months, at which point the 662 and 772 MPa data become noisy. . . . 27
15 Approximate creep strain from long-term creep tests. . . . 28
16 The 13-8 creep curve plotted on normal (not semi-log) axes. The highest stress creep curve shows the three classical stages of creep normally found during high temperature creep. . . . 29
17 Plots of creep occurring during loading below the quasi-static yield strength. . 30
18 Plots of creep in three different varieties of 304L at approximately 0.82 σ_u . . . 31
19 The Andrade equation fit to data from 304L dead-weight creep experiments. Coefficients and χ^2 values for each curve are in the boxes. . . . 32

20 The Hollomon equation as formulated by Neeraj fit to data from 304L dead-weight creep experiments. Coefficients and χ^2 values for each curve are in the boxes. 33
21 The Mott equation fit to data from 304L dead-weight creep experiments. Coefficients and χ^2 values for each curve are in the boxes. 34
22 The modified Mott equation fit to data from 304L dead-weight creep experiments. Coefficients and χ^2 values for each curve are in the boxes. 35
23 The Orowan/Nabarro equation fit to data from 304L dead-weight creep experiments. Coefficients and χ^2 values for each curve are in the boxes. 37
24 The Orowan/Nabarro equation fit to data from pure Cu dead-weight creep experiments. Coefficients and χ^2 values for each curve are in the boxes. 38

Tables

1 Experimental conditions for a series of creep and stress relaxation tests on various alloys 18

Introduction

"Creep of materials is classically associated with time-dependent plasticity under a fixed stress at an elevated temperature, often greater than roughly 0.5 T_m, where T_m is the absolute melting temperature." [1] Elevated temperature creep is taught in every introduction to materials science class and touched upon in many mechanical behavior of materials classes, so high temperature creep behavior is familiar to mechanical and materials engineers. However, the phenomenon of room temperature time-dependent plasticity in metals is much less familiar and not widely understood.

Creep can be thought of as a combination of the effects of high strain rate sensitivity and low strain hardening. A strain rate sensitive material will have a lower apparent yield stress at lower strain rates than at higher strain rates. If a strain rate sensitive material is held at a certain stress, that stress may be higher than the effective yield point at a very low strain rate. It will then plastically deform at a very low strain rate to get to the strain which corresponds to the loading stress on the stress-strain curve at that very low strain rate. However, if the strain hardening is low, the stress strain curve at that low strain rate may never have risen to the level of the applied stress, so deformation will continue indefinitely. Strain rate sensitivity increases with increasing temperature, while strain hardening decreases; therefore creep is more prevalent at higher temperatures. Strain hardening also decreases with decreasing strain rate, making the effects of creep even more apparent in low strain rate tests.

The mechanisms of low temperature (<0.5 T_m) creep are not agreed upon even by those who study creep. This report will include a review of technical literature which will summarize the experimental work done over the past 100 years to understand creep and stress relaxation at room temperature in engineering alloys. There are multiple ideas about how creep proceeds mechanistically, and similarly many theories about how room temperature creep is most accurately mathematically modeled. In particular, a master equation for describing creep in multiple alloys has been elusive. The literature review section will summarize previous work that has been done in this regard, and the description of experiments and analysis that follows will attempt to reconcile a few of the most promising equations to the room temperature creep data acquired at Sandia. It is hoped that this effort will assist Sandia's modelers in including room temperature creep in their long term predictions of alloy behavior.

Literature review

While the amount of literature that exists on room temperature creep and stress relaxation is relatively small in comparison with that which has been produced on high temperature creep, there is enough that it is helpful to divide it into categories. First in this section are the papers which merely demonstrate that room temperature time dependent deformation is occurring and try to account for it in design or experiments with minimal theorizing about operative mechanisms for the behavior.

Time dependent deformation influencing designs

Ellis et al [2] determined whether previous constitutive relationships for 304 applied to 316 stainless steel by doing cyclic tests with a combination of torsion and tension. While doing these tests they found that significant creep occurred during hold periods at constant stress. While they did not ultimately include this behavior in their constitutive relationships, they noted that "careful attention should be given to loading rate and the duration of hold periods in studies of elastic-plastic behavior at room temperature."

Pilo et al [3] investigated cyclic creep in a normalized plain carbon steel from the point of view of a mechanical designer. Engineers typically use a limit of 0.2% allowable strain in their designs, but Pilo showed that normalized plain carbon steel undergoing fatigue loading with stress less than yield stress and a positive mean stress can produce cyclic creep strains higher than the 0.2% allowed for in design.

Liu et al [4] found that small amounts (0-4%) of ferrite in 4340 steel, which do not affect the hardness or yield strength, do cause a reduction in creep resistance. In another paper [5] Liu et al. found that for 4340 with the same volume fraction of ferrite, lath ferrite creeps to a higher creep strain than massive ferrite. These papers do not actually include any arguments about why the grain morphology affects the creep, they merely state that it does.

Kassner [6] investigated the phenomena of delayed failure in silver braze joints well below their ultimate tensile strength. He concluded that the time to failure is controlled by the creep rate of silver if the base metal remains un-deformed. However, if the base metal creeps, it exacerbates the deformation in the braze joint and decreases the time to failure.

Krapf [7] wrote a masters thesis on work done to investigate stress relaxation of stainless steel rods for use in bridge pier caps. It was found that the stress relaxation at long times can be predicted from the results for shorter term stress relaxation tests and modeling.

Yamada et al. [8] did experiments to investigate the relative amounts of primary creep that occured at room temperature in several metals. They categorized their results by crystal structure, and concluded that HCP metals in general creep far more than cubic metals. The same researchers delved further into the issue in [9], finding that the creep behavior observed for Ti, Zr, and Mg do not reflect the fact that Ti and Zr undergo prismatic slip,

while Mg slips on the basal plane. There is no explanation given for this discrepancy. They also note that cold rolling prior to creep testing decreases the creep strain rate, but give no satisfactory explanation for this phenomena. In another paper [10] they extend the deformation mechanism map of annealed commercially pure titanium to include the room temperature creep regime.

Zhao et al. [11] found time-dependent deformation at crack tips in 304L stainless steel. The room temperature creep caused the fatigue crack growth rate to decrease, presumably due to a crack closure effect.

Imam and Gilmore [12] set out to prove once and for all whether creep occurs at room temperature in Ti-6Al-4V. Several authors, including Odegard and Thompson [13] had previously reported that it did occur, however Reimann [14] found that it did not occur. The result of the study was a conclusion that creep did occur in their torsional experiments and that the extent of creep strain which developed was a function of the microstructure.

Matsunaga et al. [15] studied creep in HCP metals with the goal of producing a constitutive relationship. They begin the paper with an incorrect statement that no cubic metals or alloys show creep behavior at ambient temperature below their yield stress (See [8] for one example contradicting this). They then go on to discuss creep experiments and attempts to fit constitutive equations [16, 17, 18] done in aluminum and steel, some of which was performed below the monotonic yield stress. Regardless of their inconsistency with regards to cubic metals, they used a modified Dorn equation [19] to fit the ambient temperature creep in HCP metals. The equation includes a stress exponent, activation energy, and an additional grain size exponent.

Hydrogen effects on room temperature creep

Two papers on the effects of hydrogen on room temperature creep were found. Perhaps unsurprisingly, in both papers hydrogen is found to increase creep rates. The effect of hydrogen on room temperature creep in Ti-6Al-4V was found to increase both creep strain and creep rate dramatically. [20]. The authors interpreted this to mean that hydrogen does not change creep mechanisms, but rather increases the mobility of gliding dislocations. Kivisakk [21] studied the room temperature creep in superduplex stainless steels, finding that a coarser microstructure allowed more creep to occur. They further investigated the effect of room temperature creep on hydrogen induced stress cracking, finding that creep promotes hydrogen induced stress cracking, but the presence of creep does not guarantee that hydrogen induced stress cracking will occur.

Constant dislocation density

The majority of literature papers dealing with room temperature creep mechanisms can be divided into two broad categories. One set of papers includes generation of new disloca-

tions, while the other set only includes mechanisms by which dislocations cease moving and includes nothing about how the dislocations have been generated (i.e. constant dislocation density). This section will describe the papers which assume a constant mobile dislocation density at the start of creep deformation, or at least do not include dislocation generation in their equations.

One of the earliest theoretical treatments of this idea was performed by Mott and Nabarro [22, 23]. The basis of their equation was the idea that a dislocation can pass through a potential barrier due to a quantum-mechanical tunnel effect, thus producing logarithmic creep at low temperatures.

Gupta and Li [24] did stress relaxation experiments at room temperature on zone refined niobium, tantalum, vanadium, iron, molybdenum, and tungsten as well as Fe 3.2% Si. The goal of the work was to determine the relationship between stress and average dislocation velocity, based on the idea that the rate of load drop during a stress relaxation experiments depends on the stress dependence of the plastic strain rate. All of the materials showed non-linear stress vs. log time curves and the rate of stress relaxation and total stress relaxed in a given time increased with increased prior strain rate. Counter-intuitively, the rate of stress relaxation and the total stress relaxed over time increase with decreasing temperature, although one could question the accuracy of this claim because the initial stress levels in the two experiments which are compared were different by a factor of two. This paper assumes that the mobile dislocation density remains constant throughout the tests to calculate dislocation velocity.

Barklay et al. [25] neutron irradiated tantalum alloys and compared their creep rupture behavior, finding that irradiation causes an increase in creep rupture time, and a decrease in creep rupture strain and creep rate. Based on TEM images, they concluded that this was because the dislocations in the irradiated alloys interacted with the irradiation damage and caused cross slip, slowing the creep rate.

Aluminum alloys

The creep of a rapidly solidified Al-Cr-Zr alloy from room temperature to 823 K was investigated [26] and in the low temperature range (298-523K) it was found that the activation energy of the creep rate is well matched with that of aluminum pipe diffusion. However, the exponent is too high to be associated with any diffusion-controlled dislocation creep mechanism. This is explained by the existence of a threshold stress for the start of plastic deformation at a specific temperature.

Luthy et al. [16] used torsional creep experiments to investigate high strain steady-state flow in pure aluminum. They also found a diffusion coefficient which successfully correlated with the creep data from a range of 0.21 to 0.93 T_m. However, Kassner [1], takes issue with the data below 0.4 T_m because dynamic recrystallization would have been occurring in pure aluminum under torsion. This illustrates one of many experimental problems that can occur during creep testing: it can be difficult to separate dislocation movement causing creep from

other mechanisms which may be active in the microstructure.

Hexagonal close-packed alloys (Titanium and Zinc)

Suri et al. [27] delved further into the influence of microstructure of Ti alloys on creep by growing colonies of single crystals of a near-alpha Ti alloy and subjecting them to creep. The two colonies tested had highest resolved shear stresses on different slip systems and they exhibited different creep resistances. One colony showed no dislocation pileups, suggesting that the alpha/beta interface allows dislocations to pass through. The other colony did show pileups at the interface, indicating that on that particular plane the interface provided resistance to dislocation transfer. The authors proposed a geometrical model to describe the differences in strengths, strain hardening rates, and creep behavior of the two colonies.

Miller et al. [28] found that the creep rate of Ti-6Al-2Nb-1Ta-0.8Mo went essentially to 0 after a few hours at moderately low stresses below the tensile yield strength at room temperature, with Widmanstatten alpha+beta colonies undergoing highest strains. This was attributed to their long slip lengths in the large colonies. Cyclic creep at room temperature caused creep acceleration.

Neeraj et al. [29] used the Hollomon flow equation, in which the flow stress is a function of both the strain and the strain rate, to try to describe the creep behavior of titanium alloys. When the authors compared the exponents from the Hollomon flow equation for various alloys they found that the creep time exponent was abnormally high for titanium alloys compared to other alloys. They theorize that this is due to planar deformation which leads to very low rates of local work hardening. As creep time continues in titanium alloys, the behavior deviates from the power law form. This is explained by the generation of new slip bands near grain boundaries, which propagate very slowly.

Matsunaga et al. [15] investigated the relaxation mechanism at grain boundaries during room temperature creep in pure zinc. From an Arrhenius plot which contained 5 data points, they concluded that there were two different activation energies. This is suspect since one of the activation energies was deduced from only two points, which makes a very nice line, but perhaps not a very accurate one. They make the argument that the higher activation energy corresponds to dislocation core diffusion, and the lower activation energy to 1/3 of dislocation core diffusion. The lower energy is said to correspond to grain boundary sliding, which is not activated by conventional diffusion. Grain boundary sliding and dislocation pile-up at grain boundaries were deduced from EBSD maps.

Steels

Wang [30] studied the effect of room temperature creep on the yielding behavior of a X-52 pipeline steel. After first yielding, this steel does not normally exhibit a distinct yield point on re-loading. However, after creep deformation, the yield point re-appeared. This

phenomenon is attributed to the dislocation locking effect. Larger creep deformation resulted from smaller initial loading. However, they also found that the total strain including both the initial loading and creep was insensitive to initial loading strain.

High strength low carbon low alloy steel wires were subjected to warm deformation treatments in a successful effort to decrease their low temperature creep strains and increase their low cycle fatigue lives [31, 32]. The improvement in properties was attributed to reducing the available quantity of mobile dislocations by re-dissolution of solute atoms and dislocation pinning during warm deformation.

In the 1970s some question arose as to whether the assumption of constant dislocation density during stress relaxation is correct. Rhode and Nordstrom [33] attempted to determine whether the mobile dislocation density really remains constant during stress relaxation tests by measuring whether the results of stress relaxation experiments are independent of test machine stiffness. Their results indicated that stress relaxation experiments were affected by machine stiffness, therefore mobile dislocation density must change. However, Fortes and Proenca [34] took issue with this interpretation, arguing that the difference between machines detected by Rhode [33] is caused by the materials following different deformation paths, i.e. the tests were performed at different plastic strain rates, and that no two pieces of material have the exact same initial dislocation density. Rhode and Nordstrom [35] responded to this critique by acknowledging that while the argument could be true, it cannot explain the full size of the difference between the results from the different stiffness machine.

Source activation of dislocations

The papers in this section include some description or assumption of non-constant mobile dislocation density (i.e. source activation of dislocations) during low temperature time dependent deformation.

While Li's [36] equation for transient creep was initially derived for elevated temperature creep, some authors have applied it to transient room temperature creep. The equation is based on the concept that dislocations multiply during transient creep and transient creep is exhausted either when the dislocations annihilate each other or tangle.

Shen [37] investigated transient creep in high-purity aluminum by using helicoid spring specimens. Helicoid spring specimens allow for very sensitive strain measurements. They left springs creeping over the period of a year. By this method they were able to measure steady state creep rates in the range of 10^{-10} to 10^{-12} /s. They used Li's equation [36] to fit the creep curves. Steady state creep rates for water quenched material were found to be an order of magnitude smaller than that observed in air quenched material. They use this evidence to state that the creep is controlled by recovery and hardening mechanisms.

Schmidt and Dietrich [38] attempted to correlate the yield stress from a room temperature tension test with the room temperature creep limit and the strain hardening coefficient with the creep resistance. The creep tests were only performed for 15 minutes. Yield stresses and

creep limits were compared both amongst various steel, titanium, and aluminum alloys and with various amounts of cold work in one steel alloy, finding no concrete relationship between them. They also demonstrated that in steels in which the strain hardening coefficient changes with deformation, the creep rate also changes. This result could have been predicted from the premise that dislocation motion is what governs creep. Work hardening can be simply thought of as dislocations gradually ceasing to move, generally by becoming tangled. If this is likely to occur in an alloy, then dislocation movement during creep is also likely to be hindered, giving the alloy higher creep resistance. However, in the case of yield stress, which can simply be conceived of as the point at which many dislocations begin to move, the logical conclusion would be that lower strength alloys should have a higher creep rate, because dislocations are more easily moved. However, this is not always the case, indicating that some other mechanisms are active. Perhaps the strain hardening rate effect (tangling) overwhelms the yield strength effect (movement/generation). Given the work in this paper on strain hardening, perhaps it would have made more sense to include that study with the yield strength to better understand the creep rate trends.

Miller [39] performed room temperature creep tests on die cast AZ91 magnesium. He concluded that diffusion-driven dislocation climb may be the rate controlling mechanism for creep above 120MPa at room temperature, but that creep below 120 MPa seems to have a different activation energy and therefore creep mechanism. No speculation as to what that mechanism might be is included.

Room temperature creep of tantalum tritides [40] was attributed to stress induced dislocation loop action which punched through bubbles of helium in directions close to the stress axis.

Matsunaga et al. [41] made an effort to re-write the deformation maps for pure Cu, Al, and Pb, all FCC materials. The findings, which were based on activation energy arguments, caused the authors to theorize that the relatively high stacking fault energy in aluminum causes cross-slip, which means that creep deformation proceeds though dislocation creation at Frank-Reed sources, and is controlled by cross slip. In copper (low stacking fault energy), the creep is thought to proceed through dislocation glide because cross-slip is less favorable.

Titanium alloys

Zeyfeng [42] investigated creep in titanium at room temperature and below with the goal of understanding the rate limiting mechanisms, coming to the conclusion that the rate controlling process is thermally activated overcoming of dislocation barriers associated with interstitial atoms.

Thompson and Odegard [43] considered creep in Ti-5 Al-2.5 Sn on several samples with varying processing histories. They found that while creeping at 90% of the tensile yield the samples all behaved in the same manner. However, during creep at 60% σ_y the changes in processing history made a difference in the creep response. They proposed two reasons for this behavior: First, they suggested that the different processing histories lead to different

quantities or strengths of obstacles to dislocation movement. However, the calculated activation energy and the initial microstructures, which were very similar in all three samples, did not support this conclusion. The second argument is based on ease of dislocation source operation, theorizing that the various processing paths resulted in dislocation sources that activated at different stresses. TEM examination of the post-creep microstructures provided further evidence for this second explanation. Odegard and Thompson [13] also worked further on creep in Ti-6 Al-4 V, finding that pre-straining the material reduced the amount of creep that occurred. Additionally, they found that the welded material crept more, and that the rationalization proposed in [43] for Ti-5 Al-2.5 Sn held true for Ti 6-4.

Savage et al. [44] investigated the phenomenon of creep recovery, which is reversal of creep strain after unloading, in titanium alloys. After initial creep has reached steady state, the material is unloaded and left in an unloaded state at room temperature for some period of time from 24 hours to 11 months. When creep recovery occurs, the material exhibits the same initial creep curve upon re-loading as it did in the first loading cycle. They found that this phenomenon occurred in air cooled samples, but not in ice water quenched samples, as well as in samples oriented to maximize the resolved shear stress on the a2 basal slip system, but not in samples oriented so that the a3 basal slip system was active. Based on these observations, the authors propose that the creep recovery is due to the relaxation in the internal stresses that arise due to the interaction of planar slip with grain boundaries or alpha/beta interfaces. The relaxation in internal stresses can generate new dislocation sources, which are then active on the second loading. For beta alloys, or the samples oriented for a2 basal slip, the dislocation pileups are within the beta phase, making the recovery mechanisms much more difficult. This is consistent with the results described by Suri et al. [27].

Oberson et al. [45] found through SEM and TEM analysis that slip and twinning are the active deformation mechanisms during creep in alpha-Ti-1.6V in the temperature regime from room temperature (0.15 T_m) to 0.25 T_m. At low strain levels, they found the activation energy for creep to be close to the activation energy for slip, while at high strain levels the activation energy does not match either slip or twinning, suggesting that they work together. They theorized that twin nucleation is caused by dislocation pileup, which causes the twins to become active after a certain strain threshold is reached. Increasing oxygen content and decreasing grain size inhibit twin growth [46] and therefore should be helpful in decreasing the creep strain.

Steel alloys

Krempl [17] studied the uniaxial viscoplastic behavior of 304L stainless by short term creep and stress relaxation experiments at room temperature. He found that the relaxation behavior depends only on the strain-rate preceding the relaxation test, not on the strain magnitude. Under cyclic loading conditions, the work hardening and also the change in strain rate sensitivity are active, while in monotonic loading only work hardening is active. Based on this, the conclusion is reached that "creep, relaxation, and rate sensitivity still have

the same form but are changed in magnitude after cyclic loading." Kujawski and Krempl [47] performed further tests to confirm their findings in [17], pointing out that one source for discrepancies between creep or relaxation data from different authors is the influence of prior loading rate, which is not often reported. They extended their studies to a Ti alloy [48], finding that the same behavior applied, but in larger magnitude than the 304 stainless. In FCC metals, strain rate dependence is thought to be governed by thermally-activated release of dislocations from local pinning points, and it manifests mainly as a change in strain hardening rate [49]. From this perspective, it makes sense that the relaxation behavior would depend on the previous loading rate, because that is what governs the number of dislocations active in the material. In the case of the Ti alloy, some HCP materials have also been found to exhibit the same response to changes in strain rate as FCC metals, so the same argument applies. The findings in regards to cyclic straining changing the work hardening also can be attributed to the amount of available dislocations for thermally-activated release from local pinning points changing as the material is cycled.

Alden [50] states that permanent deformation consists of both a plastic component and viscous component, the viscous component being composed of many small strain increments caused by thermal activation of dislocations exceeding energy barriers. His next paper [50], makes the point that the stress rate applied during loading 304 stainless steel strongly influences the creep strain, which agrees with Krempls work [17, 47]. This is interpreted to mean that mobile dislocations nucleate with increasing stress, they move, then they get trapped in a network. His final paper on the subject [51] applies the same arguments to a variety of metal systems. The conclusion in this paper is that viscous drag (frictional resistance) to dislocation motion makes materials have different yield stresses and different creep behaviors. While evidence of this effect has been shown in several of the other papers reviewed here, it seems to leave out the dislocation generation/unpinning part of the mechanism that was discussed in his first paper [50]. Henshall and Miller [52, 53] also worked on unified constitutive equations for creep and plasticity based not only on thermal activation of dislocations, but also on stress activation. In part II of the paper [53] they verify the model only with pure aluminum and an Al-Mg alloy. By 1990 there was quite an abundance of data on other alloys (Ti and various steels, for example) it is curious that they did not include different chemistries.

Oehlert and Atrens [18] wrote a comprehensive article on "Room Temperature Creep of High Strength Steels." The primary creep mechanism was identified as pure dislocation creep. Krempl [17] had previously found that the accumulated creep strain in stainless steel was dependent on the applied load and loading rate, however in these high strength steels the creep strain was only dependent on the applied stress. Additionally, a unified creep model which describes the primary creep in the high strength steel alloys eluded the authors. All of the alloys showed logarithmic dependences between creep strain, strain rate, and applied stress, but their behaviors were different from each other. If the high strength alloys which Oehlert and Atrens tested exhibit less strain rate sensitivity than 304L which Krempl looked at, this result may be explained at least in part by the fact that changing the strain rate does not change the amount of dislocations which are active to the same degree as it does in 304L. Comparing data for strain rate sensitivity of 4340M and AerMet100 [54] with data for strain

rate sensitivity for 304L [55], 304L's yield strength increases by a factor of approximately 1.55 from 0.0001 1/s to 100 1/s strain rate, while Aermet 100 and 4340M only increase by factors of 1.05 and 1.12 respectively over the same range. Additionally, Aermet 100 and 4340M show increases in their ultimate strengths, while 304L shows a decrease in its ultimate strength. These differences are due to the differences in crystal structure and strengthening mechanisms amongst 304L (FCC austenite, strain hardened) and 4340M (BCT martensite, quenched and tempered), and AerMet100 (BCT martensite, precipitation hardened).

The creep behavior of several heat treatments of carburized 4320 steel at room temperature was studied [56], and a model for the deformation was proposed. The model was able to characterize the logarithmic creep behavior while explaining the anisotropy of the creep strain components by relating it to the deviatoric stress.

Tendo et al. [57] studied the effects of solute carbon and nitrogen on the creep of austenitic stainless steels at room temperature. Nitrogen increased the logarithmic creep strain while carbon had no effect. The steels with added nitrogen showed planar dislocations and dislocation pileups unlike the pure steels and carbon containing steels. The authors theorized that dislocation pile-ups cause stress concentrations which speed the movement of dislocations.

Cyclic loading

Yang et al. [58] studied cyclic creep behavior in commercially pure aluminum at room temperature. Grain size was found to affect the creep rate dramatically. One mechanism of high temperature creep is grain boundary sliding, which causes material with smaller grains to creep faster at high temperature. However, in this case the mechanism is different. They also found a threshold stress where cyclic creep retardation changed to cyclic creep acceleration, and linked this threshold stress to impurities in the material. This behavior was explained in terms of thermally activated dislocation movement. In a very similar paper, Ishikawa et al. [59] studied creep behavior of high purity aluminum at room temperature. It was found that steady-state creep could be observed at room temperature, with the creep rate depending upon the applied stress. Applying cyclic stress accelerated the creep rate and the creep rupture. Ishikawa et al. [60] later repeated earlier work [59] with even purer aluminum (99.999% Al), finding that steady state creep had not stopped occurring in pure aluminum since the work five years earlier. However, this time Voigt and Maxwell spring and dashpot models were employed to mechanically model the creep behavior. Based on these models, it was hypothesized that the material has a dual composite structure, with one hard phase and one soft phase. Contrary to the normal use of the word phase, which implies separate crystal structures, the researchers found that the hard "phase" was the subgrain boundaries where dislocations piled up, and the soft "phase" was the interior of the subgrains. This was verified by TEM.

Evans and Parkins [61] performed cyclic creep tests on a C-Mn steel, finding that load cycling accelerated the creep process in comparison with static loading. They posit that the creep acceleration is due to reverse movement of dislocations during the unloading part of the

cycle which accelerates dislocation movement. Bennett and Evans [62] used copper to further investigate Evans previous observations on cyclic loading [61]. They found two stages of what they called "induced creep" were present, the first stage of which has decelerating creep. The second stage, only present at higher stresses (but still below the monotonic yield stress), was characterized by accelerating creep. Included in this paper is a very thorough and well-thought out argument for how dislocation movement can account for these two very different stages. The backward movement of dislocations cited in [61] is further supplemented with cross slip of screw segments and the effectiveness with which the cross-slipped dislocations can provide new strain sources. The second stage occurs when vacancies produced by the plastic deformation in the first stage can induce climb of edge dislocations, possibly along with other unknown processes to make the creep faster.

Wang and Chan [63] also studied the effects of combinations of cyclic and static loading on the creep deformation of the X-52 pipeline steel. They found that a low number of cycles preceding a static creep hold resulted in smaller cumulative creep than pure static creep, but that a high numbers of cycles preceding a static creep hold resulted in very high creep rates for short periods. This is somewhat analogous to the work by Yang et al. [58], except that in that case the level of stress was changed rather than the number of cycles. They explained this phenomenon by proposing that cyclic loading causes dislocation cells to form, which hinder dislocation movement. Therefore, cyclic loading will result in less creep than static loading. However, they theorize that these dislocation cells which are in a quasi-static state during cyclic loading, may destabilize and collapse, contributing to the high creep rates for short periods. They state that if the number of cycles is small, the hardening is predominant, but with more cycles, the collapse is dominant. The only evidence for this explanation outside of the creep data is the observation of more slip lines on the specimen surface after cyclic creep than after static creep. In the Yang paper [58], the acceleration of creep had been linked to a threshold stress caused by impurities in the material.

Experimental procedure

Experiments were conducted on nine different alloys on four different test systems, with three different strain measurement devices to confirm that creep at room temperature which was being observed was not a function of experimental setup. The creep tests were programmed to proceed under load control to 0.1% strain at 2 lbs/sec, hold at that load for 10 minutes, then go to 3% strain at 2 lbs/sec, then hold for 10 minutes, continuing on in the same fashion for 6%, 9%, and 12% strain. The stress relaxation test proceeded under strain control to load to 0.1%, then held at that strain for 10 minutes, continue loading at 3.3×10^{-6} sec^{-1} to 3% strain, hold for 10 minutes at that strain, continuing in the same fashion for 6%, 9%, and 12% strain. The sizes of the samples and extensometers used for each test are listed in Table 1.

Table 1. Experimental conditions for a series of creep and stress relaxation tests on various alloys

Material	Cross section dimensions (mm)	Gage length (mm)	Extensometer	Type of test
2024-T3	12.7 x 17.78		1/2", 15%	creep
Copper	1.45 x 1.07	5	± 1.5 mm	creep
Tantalum	1.52 x 0.97	5	± 1.5 mm	creep
Nitronic 50	6.32 x 3.28		1/2", 15%	creep
Cast 304L	6.32 x 3.20		1", 50%	creep
304L	6.32 x 3.14		1/2", 15%	creep
Ta-10W	6.20 x 2.06		1/2", 15%	creep
17-4	6.30 x 3.12		1/2", 15%	creep
13-8 Mo	6.32 x 3.20		1/2", 15%	creep
Ta-10W	6.22 x 2.05	12.58	1/2", 15%	relaxation

To confirm that possible movement or vibration from the hydraulic systems used to conduct the tests listed in Table 1 was not causing the creep and stress relaxation effects observed at room temperature, simple dead-weight tests were performed on a number of wires. In these tests, a wire was wrapped around a fixed bar several times, the end secured by twisting it around itself, or with tape. Reflective tape flags were attached to the wire, and a laser extensometer was used to track the strain. The bottom of the wire was attached to a metal hanger on which weights could be placed. Weights used for calibrating load cells were placed on the hanger, and the creep rate was recorded with the laser extensometer. 0.254 mm (0.010") 304L wire and 1.27 mm (0.050") pure Cu wire were tested in this manner.

As discussed earlier, whether or not room temperature creep saturates after some time is a matter of dispute. To measure this, a dead-weight experiment was set up in a similar fashion to that described above. Four 304L wires approximately 1.2 m long were hung on a steel tube. Black tape flags were affixed near the top and bottom of the wires, and various weights were hung to achieve stresses of 641, 703, 758, and 793 MPa stresses in the respective

wires. A camera was set up so that the field of view included the entire assembly, and pictures were taken at fixed intervals. Figure 1 shows the wires before loading, within 1 minute of hanging the weights, after 24 hours, and after 3 months. The resulting images were analyzed to determine the strain in each wire. Some difficulty was caused by lens imperfections which changed the measurements of length if the angle of the camera was adjusted. As this experiment proceeded for a year in an active lab, the camera was inadvertently moved several times, and the change in scale caused by the change in camera position was accounted for by normalizing the length of the wire between the markers by a length measure taken off of the measuring tape hanging to the right of Figure 1.

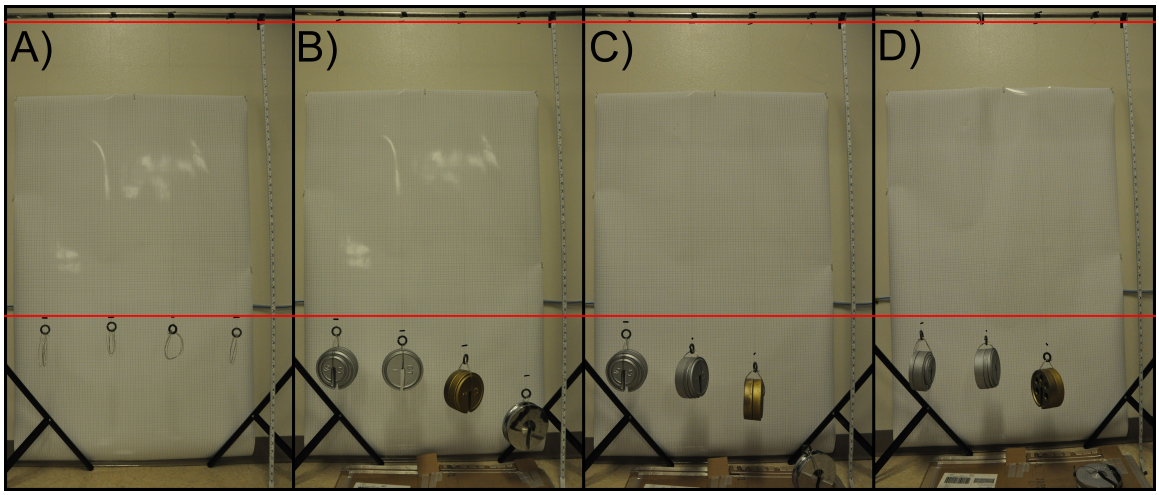

Figure 1. Long term dead weight tests: a) before loading, b) within one minute of loading, c)24 hours after loading, d) 3 months after loading

In addition to the creep tests described above, uniaxial tension tests were performed on all alloys. In order to calculate approximate creep strain, the stress at which each creep test was started was correlated to the strain from the uniaxial tension test at that stress, and that "instantaneous strain" was subtracted from all of the strains.

Results

The results of the successive loading dead-weight creep tests showed that creep was occurring at room temperature in the 304L and pure copper. Figure 2 includes the total strain produced from the successively increasing loads on the 304L sample. The sample failed at the end of the plotted data, during creep at 878 MPa. The creep curves for the pure Cu and 304L wire are similar (Figures 3 and 4), with logarithmic creep occurring up to a certain stress. At higher stresses the creep begins to accelerate. In both the 304L and Cu curves displayed, the sample failed at the end of the final creep curve plotted.

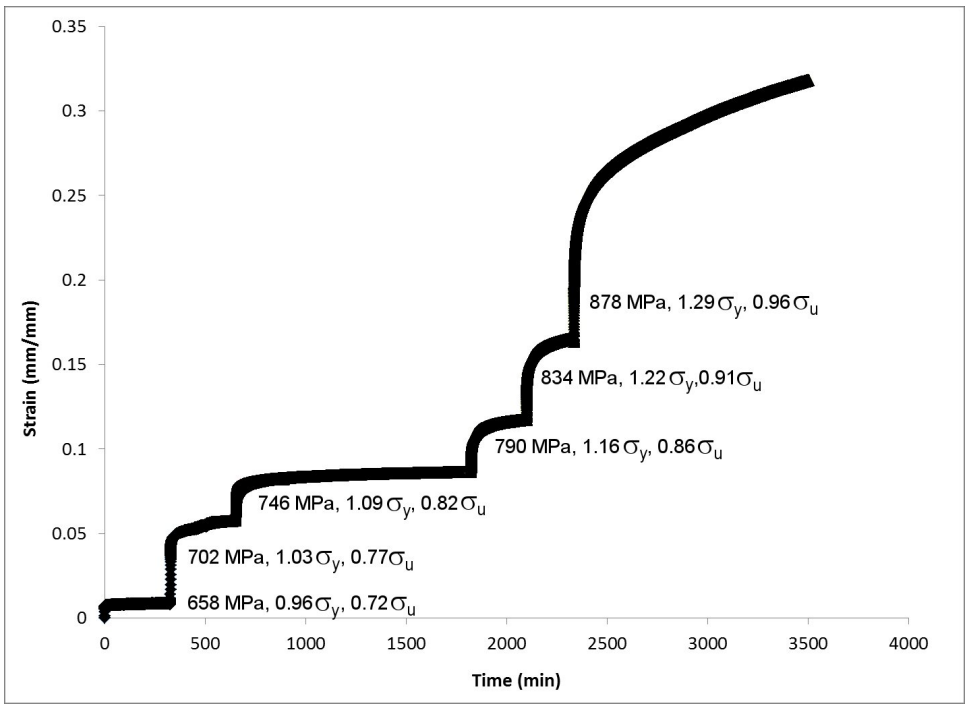

Figure 2. Total strain caused by a multiple load creep test on 304L wire.

The ten-minute creep curves obtained from the tests performed on several alloys with the various test systems detailed in Table 1 are plotted in Figures 5-13. The Ta-10W sample, 17-4 sample, and 13-8 sample each ruptured during the final creep curve that is plotted.

Figure 14 is a plot of the total strain, including the elastic and instantaneous plastic strain which resulted from the long-term creep tests on 304L wires. Figure 15 is a plot of the approximate creep strain, which was calculated by subtracting the strain from a quasi-static stress-strain curve that corresponded to the loading stress. Both are included for completeness.

The 876 MPa sample failed at nearly exactly 24 hours after loading. The data for the 710 and 772 MPa curves are fairly smooth, straight lines until the 3 month point. The 662 MPa

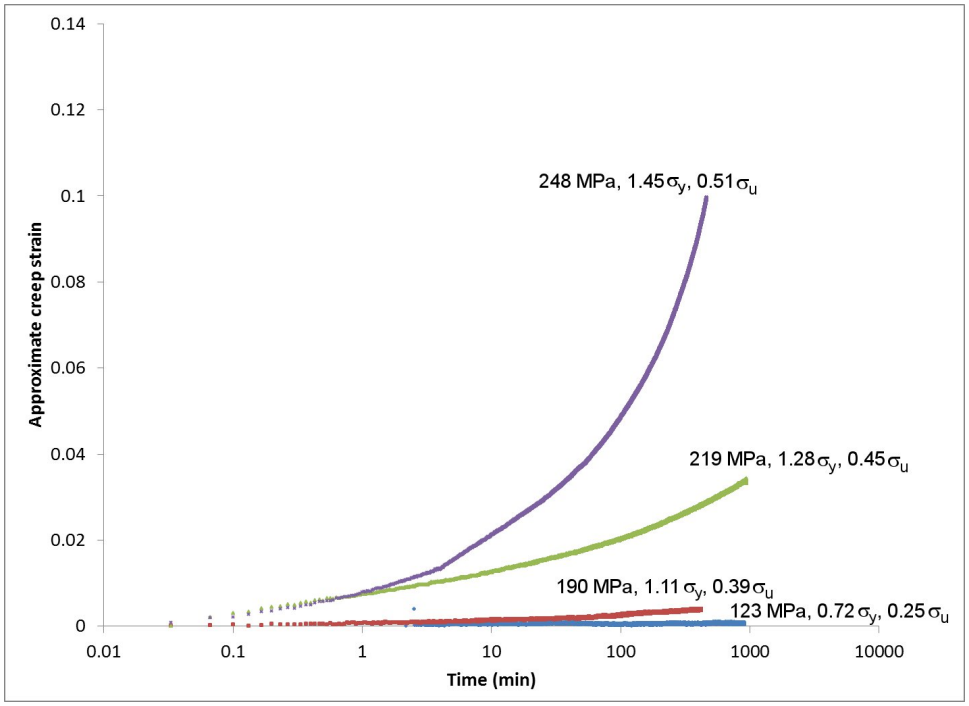

Figure 3. Pure Cu wire creep curves at various loads

data seem to increase in rate suddenly after the 1 day mark. What causes this is unknown, but the jump in rate is not due to a shift in camera or other experimental error. The sudden increase in strain at the 3 month mark is thought to be due to camera movement, not actual strain in the 662 MPa sample. After the 3 month point, the data becomes noisier and more difficult to interpret. It does appear to have a continual slight upward slope, indicating that creep is continuing, but the value of that slope is difficult to extract because of the noise in the data.

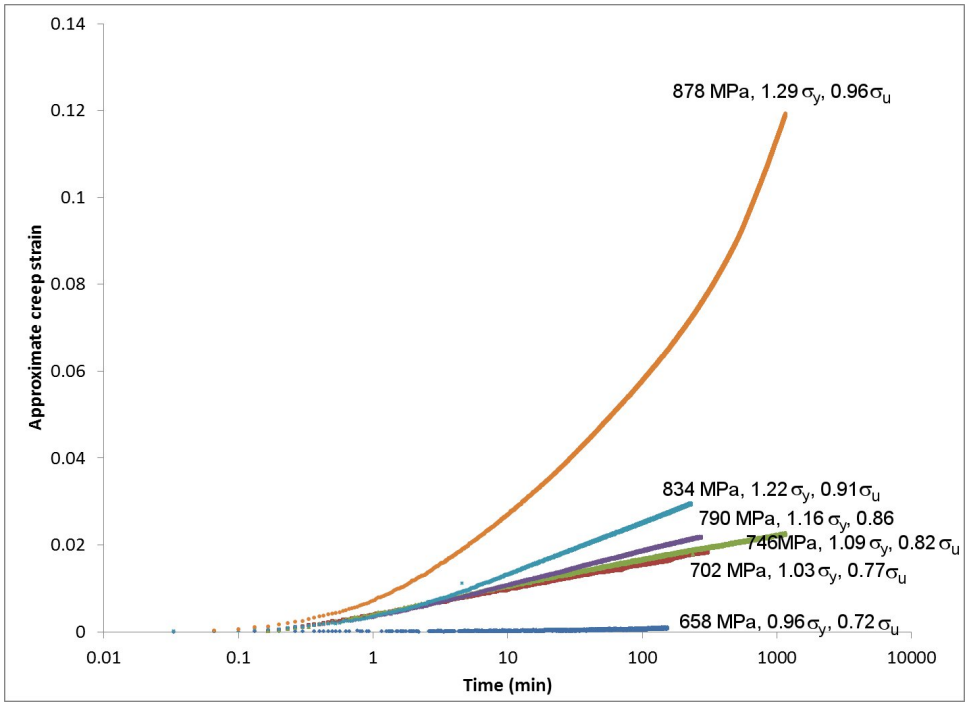

Figure 4. 304L wire creep curves at various loads

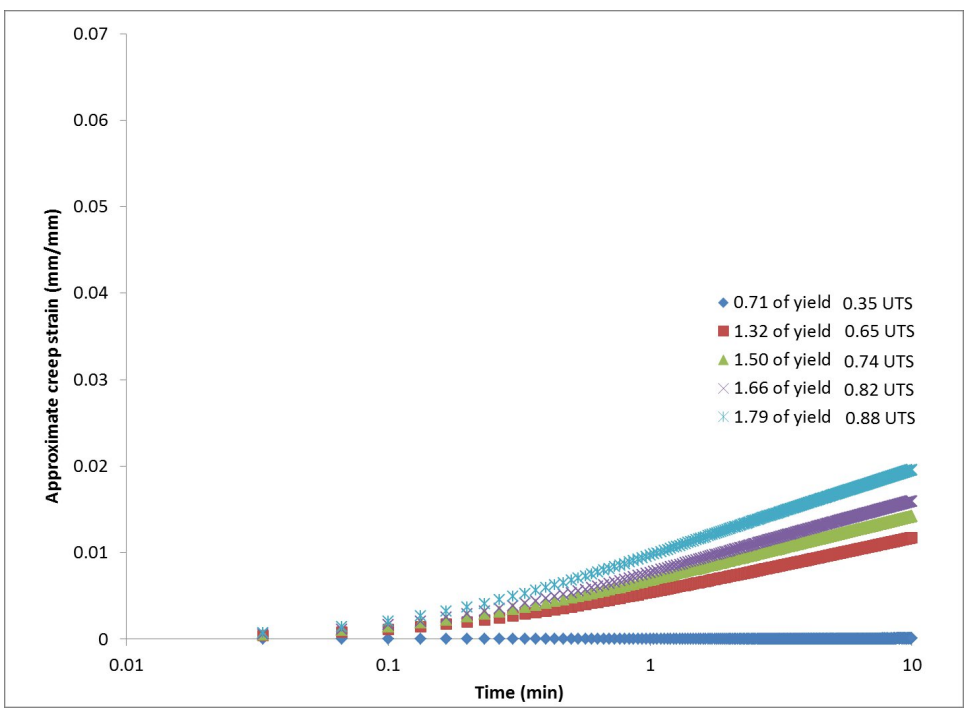

Figure 5. Creep curves on a wrought 304L tensile sample

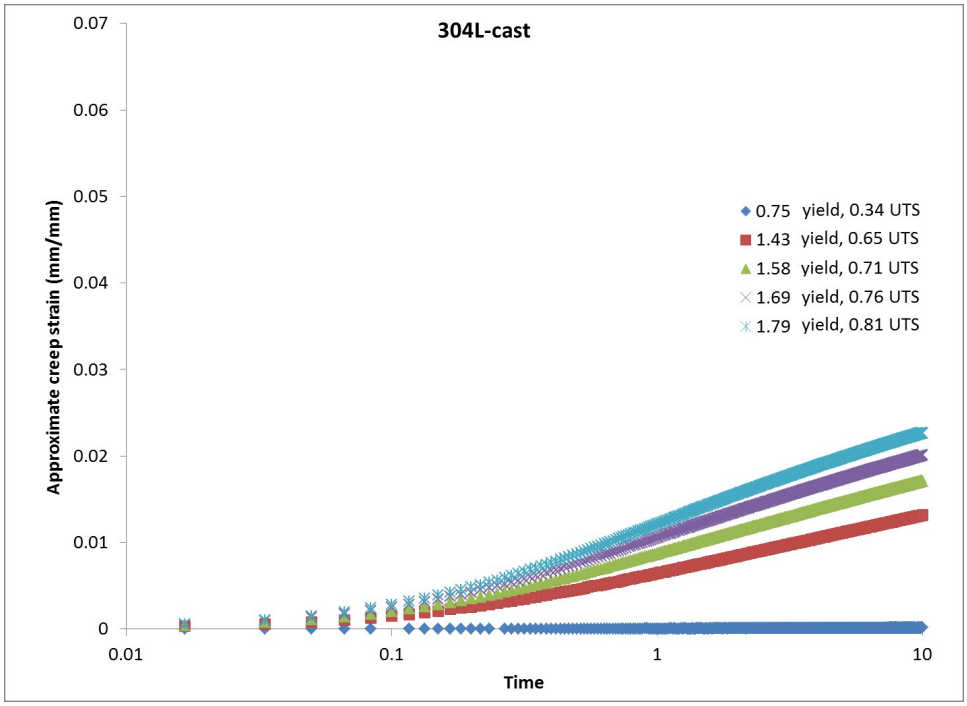

Figure 6. Creep curves from a cast 304L tensile sample

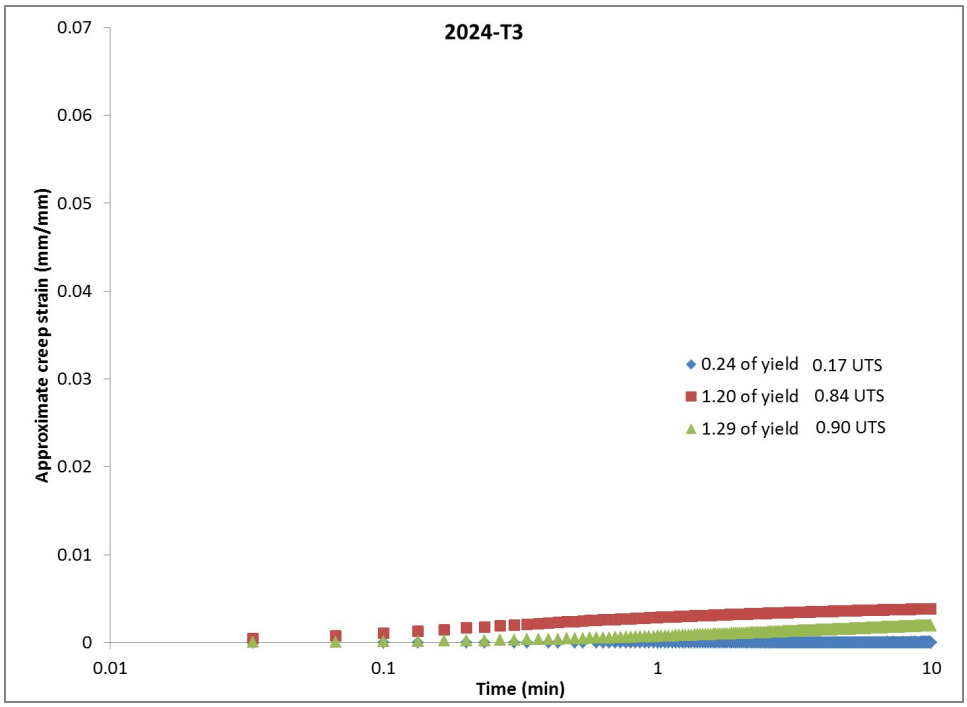

Figure 7. Creep curves from a 2024 Al sample

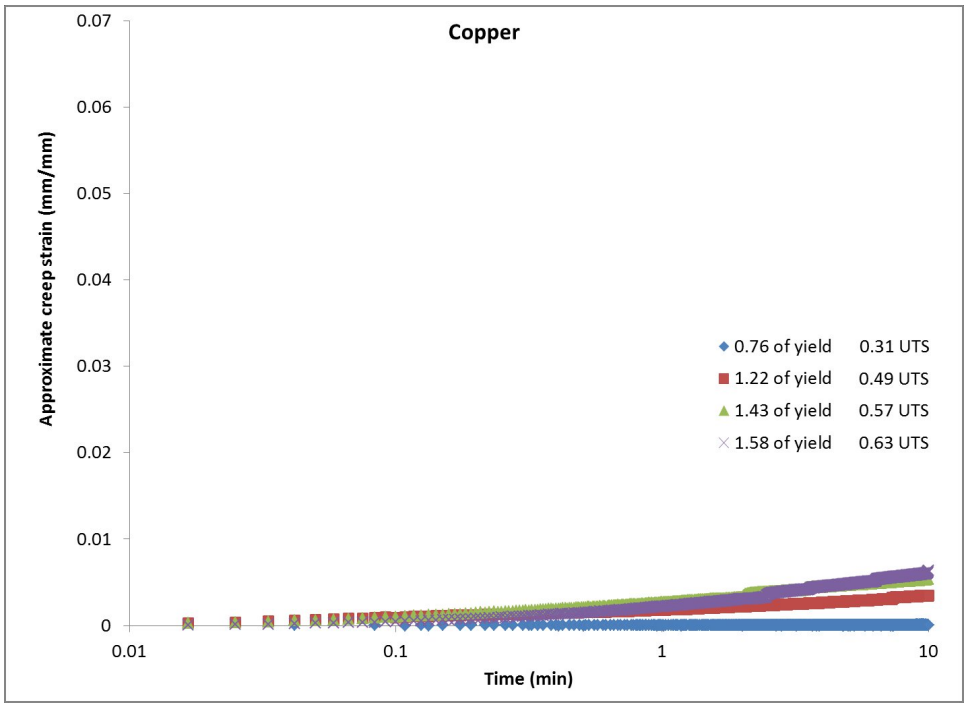

Figure 8. Creep curves from a pure Cu sample.

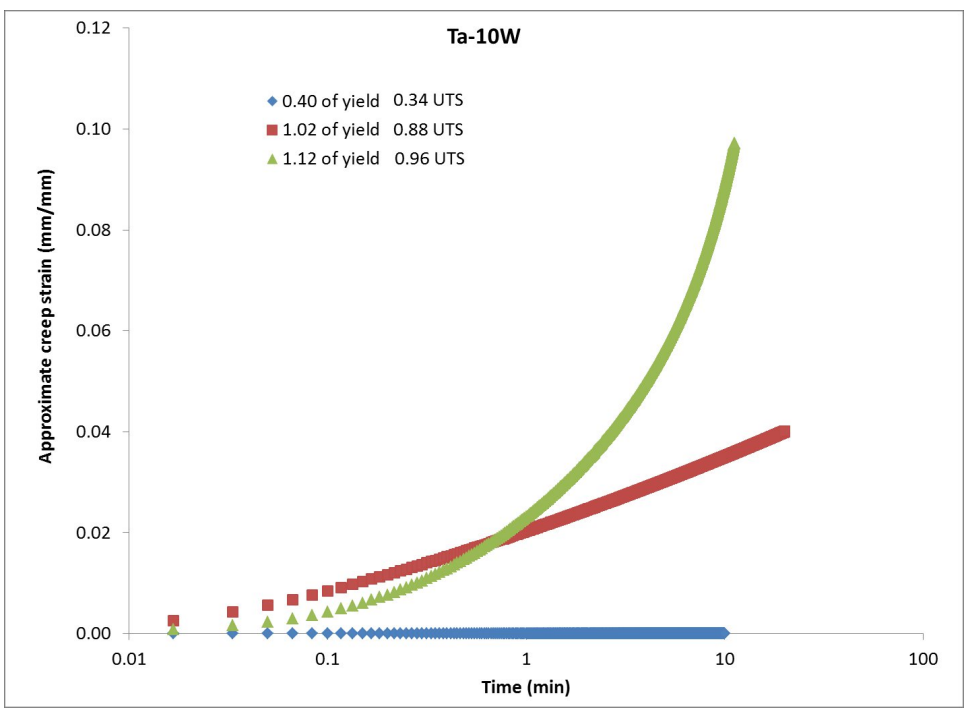

Figure 9. Creep curves from a Ta-10W sample

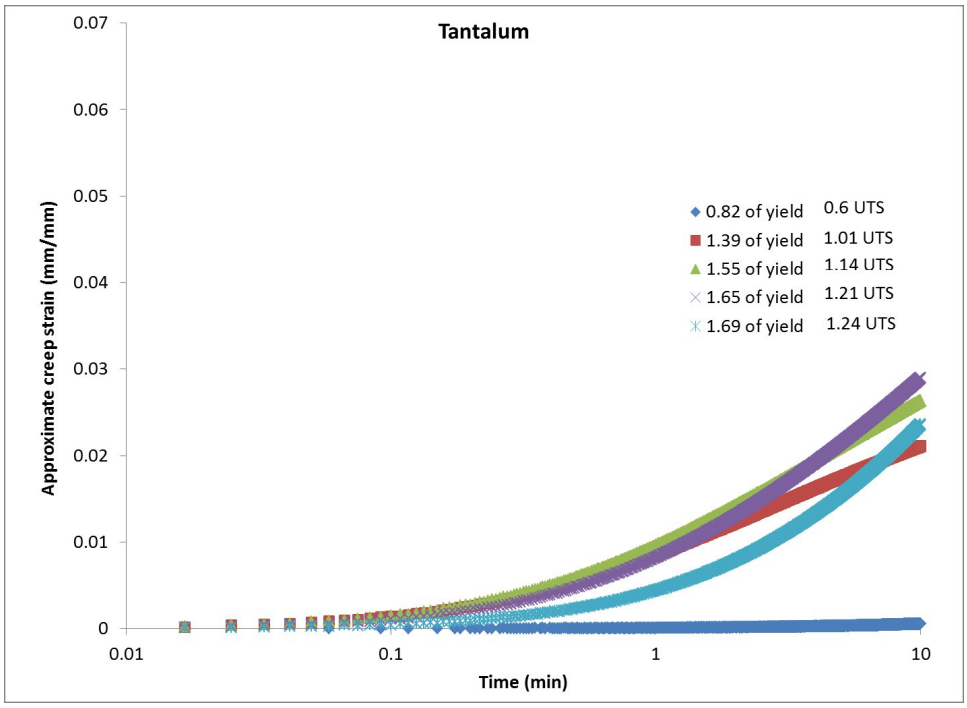

Figure 10. Creep curves from a pure Ta sample

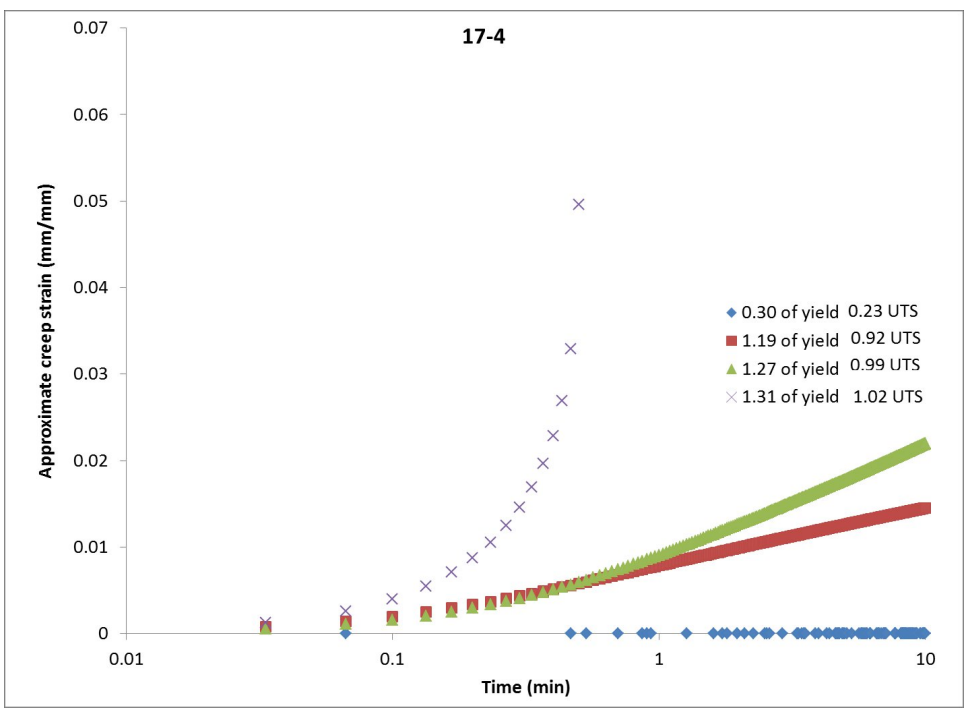

Figure 11. Creep curves from a 17-4 sample

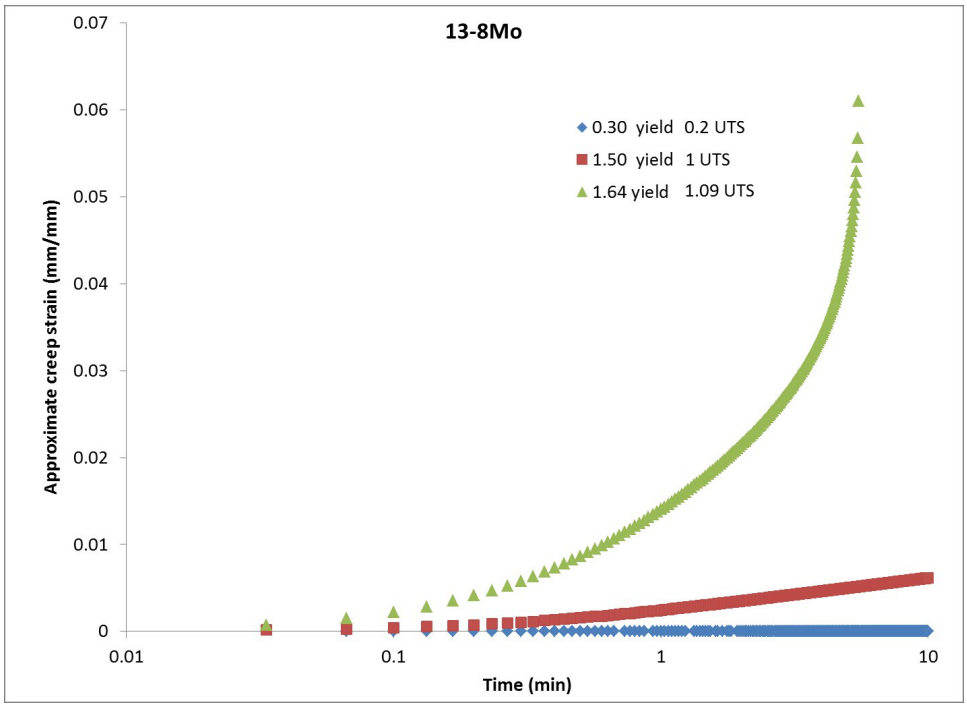

Figure 12. Creep curves from a 13-8 sample

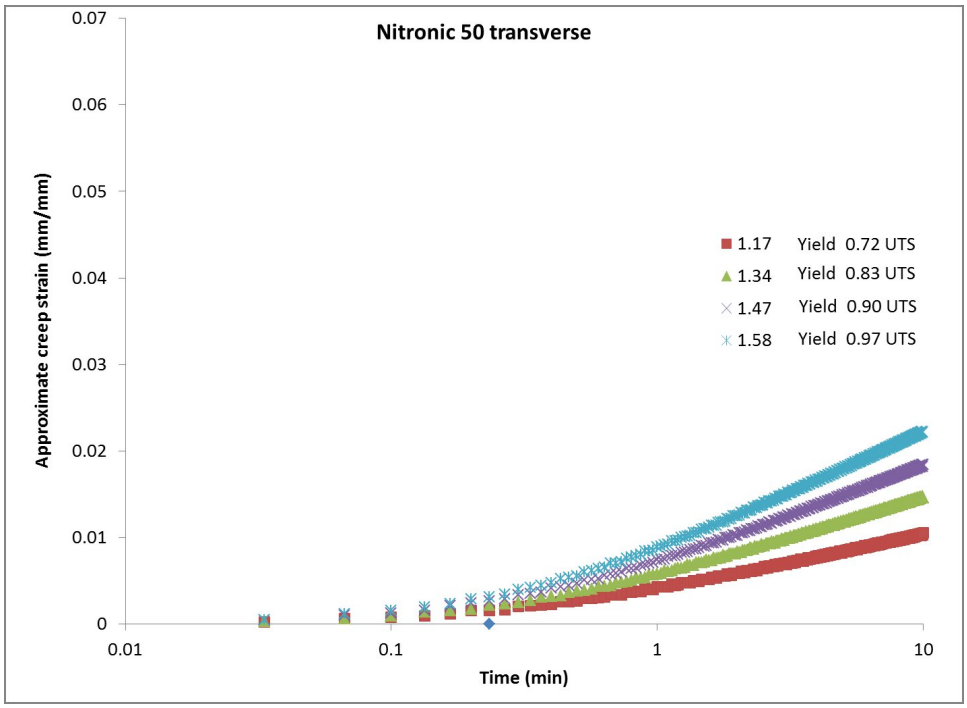

Figure 13. Creep curves from a Nitronic 50 transverse sample

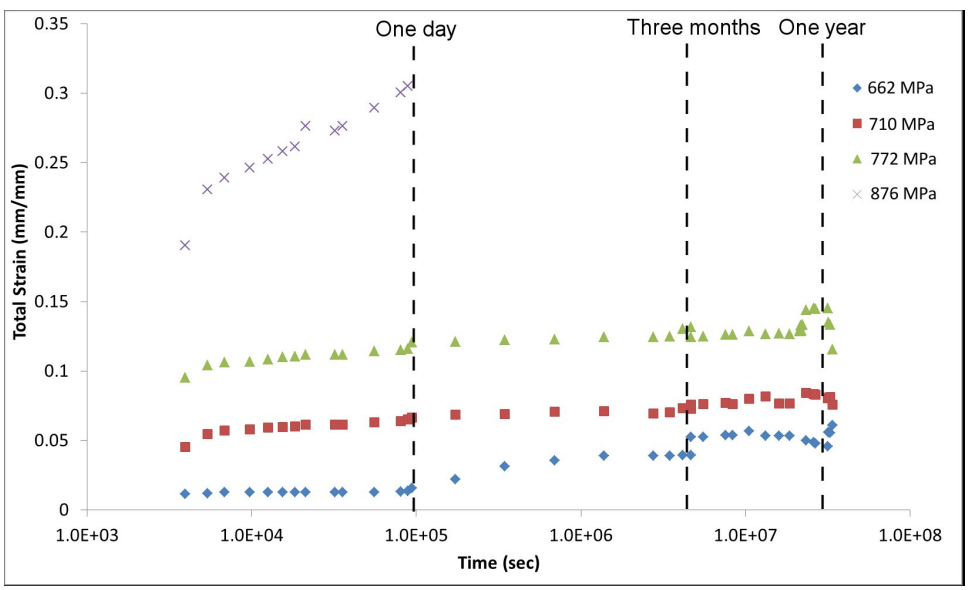

Figure 14. Total strain (including instantaneous strain) from long-term creep tests. Data is well-behaved up until about 3 months, at which point the 662 and 772 MPa data become noisy.

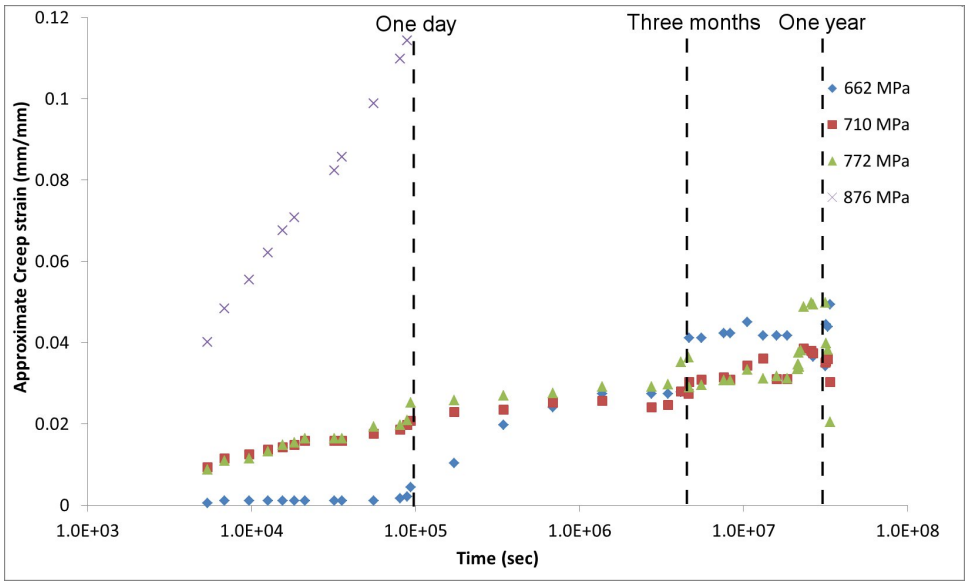

Figure 15. Approximate creep strain from long-term creep tests.

Discussion

Observations about the creep data presented in the results section

The creep data collected for this report shows that here is a distinct threshold stress over which creep proceeds in a non-logarithmic manner. The threshold stress where the non-logarithmic behavior begins does not seem to correlate to any specific fraction of yield or ultimate stress that is consistent among the various alloys. It does remain consistent from test to test within the same alloy (304L dead weight vs. long term test). In the case of the 13-8 sample, this non-logarithmic behavior in the highest stress experiment, if plotted on a normal (not semi-log) plot as in Figure 16, can be seen to be the classic shape of a high temperature creep curve showing primary, secondary, and tertiary creep regions. With the exception of the 17-4, the other samples which showed evidence of non-logarithmic creep under high stress did not show evidence of tertiary creep before failure. The 17-4 sample failed very rapidly (within the first minute) and showed only accelerating creep over that period of time.

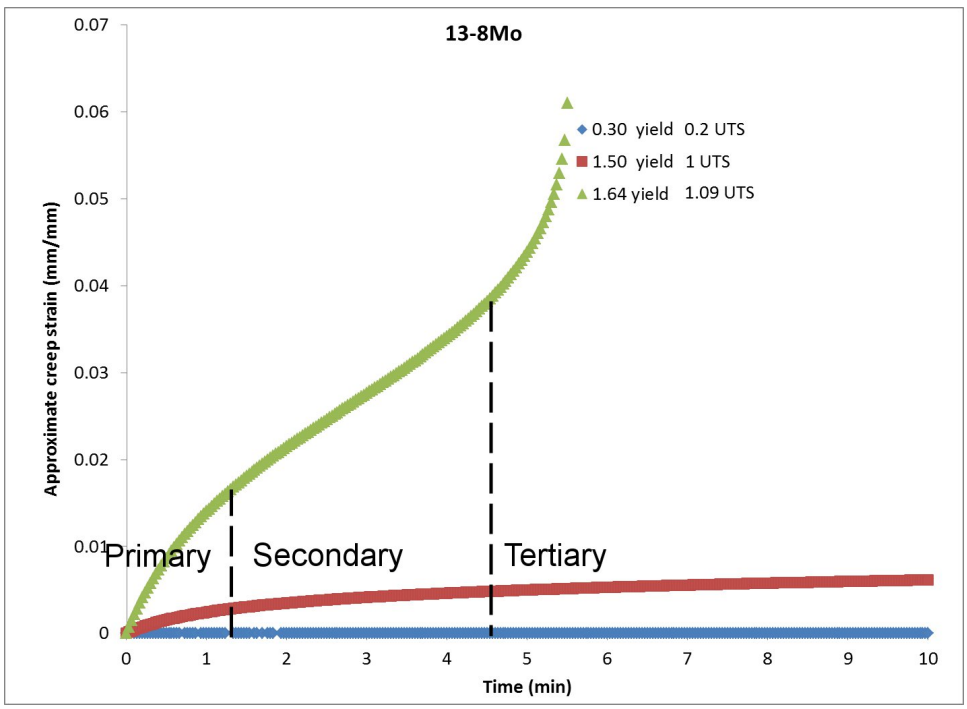

Figure 16. The 13-8 creep curve plotted on normal (not semi-log) axes. The highest stress creep curve shows the three classical stages of creep normally found during high temperature creep.

Creep at room temperature in the alloys studied occurs even at loads which are below yield strength. Figure 17 plots data from tests performed at stresses below the quasi-static

yield stress on the same axis. It is evident that there is more scatter in some sensors used than others (Cu and 304L at 0.96 σ_y have a lot of scatter), but the slope of all of the curves are positive. While some sensor drift could be expected, and might be argued to contribute to some of the very small strains, it seems unlikely that the drift would both so uniformly positive and so evident over a period of only 10 minutes. In the future, whatever extensometer is chosen for creep experiments should be monitored in the environment in which the test will be performed while fixed at a known strain to determine the amount and character of any sensor drift. The creep rates of the Ta at 0.82 yield and 304L at 0.96 yield appear to be constant or accelerating rather than decreasing even at this low fraction of yield. It is unlikely that this is an experimental artifact, as the Cu samples at 0.76 of yield were tested with the same experimental setup as the Ta sample (see Table 1) and do not show such a rise in creep rate.

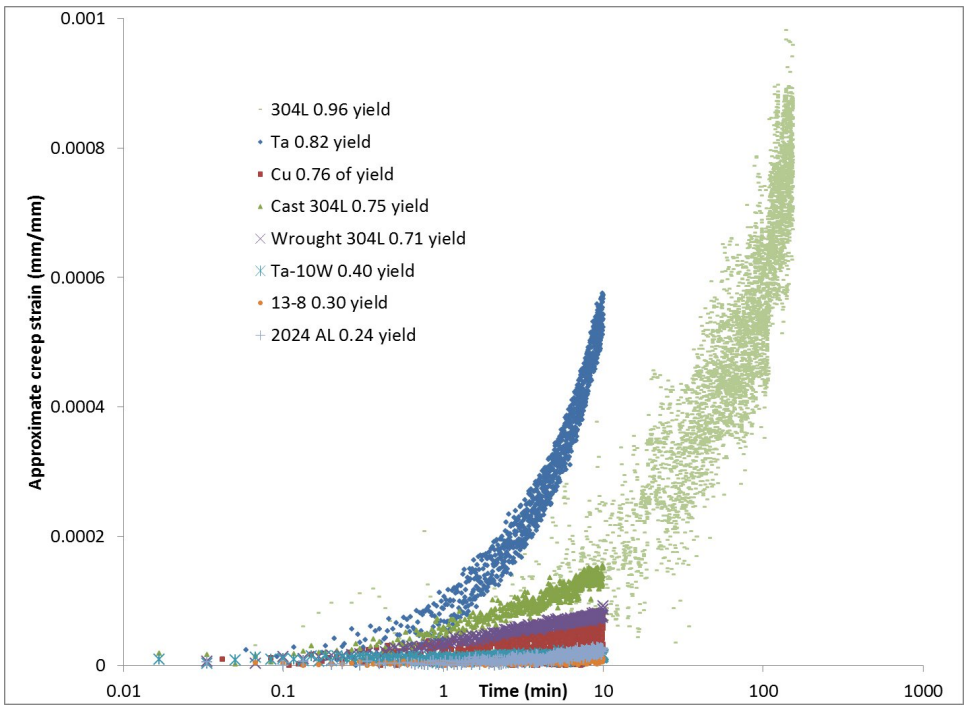

Figure 17. Plots of creep occurring during loading below the quasi-static yield strength.

Several observations can be made about the long-term creep experiments in 304L wire. First, the behavior of the 710 and 772 MPa creep curves are very similar, and distinctly different both from the 662 MPa creep curve and the 876 MPa creep curve. In the context of Sandia's applications, likely the lowest strain is the most relevant, because components are generally designed to function within the elastic regime. With this in mind, the source of the curious acceleration of creep after a period of one day in the 662 MPa sample should be further investigated. Second, all three curves do appear to have a continuous positive slope, indicating that creep does not saturate, at least over the course of a year. Although on a

semi-log plot a positive slope indicates a logarithmically decreasing strain rate, it remains important because it implies that creep could continue throughout the lifetime of a NW component, where it may eventually add up to enough deformation to cause a problem. Even in the lowest stress wire, the total strain after one year was approximately 5%, which is not negligible. Third, while the simple method of this experiment was useful for a first examination of long term creep, a method with better strain measurement capabilities that is less easily disturbed by everyday lab activities would be advisable in the future.

Three varieties of 304L samples were creep tested in this set of experiments. A wrought 304L, a cast 304L, and the drawn 304L wire. The 304L wire was drawn to a very high strength, therefore there should be a very high density of dislocations interacting to cause the high strength. Although the processing history for the wrought and cast 304L is unknown, as-cast 304L is likely to have fewer dislocations than the wrought material. A comparison of the creep strain in the three materials at approximately 0.82 σ_u is provided in Figure 18. The cast 304L, which has the lowest strength, creeps the most, while the wrought 304L with the highest strength creeps the least. Because there are so many dislocations already present in the wire, mobile dislocations will be more likely to be arrested by interaction with stationary dislocations. Unfortunately, the prior deformation history of these samples is not known, so the data cannot be checked against the theory that the strain rate of prior deformation influences the creep strain [50, 17, 47].

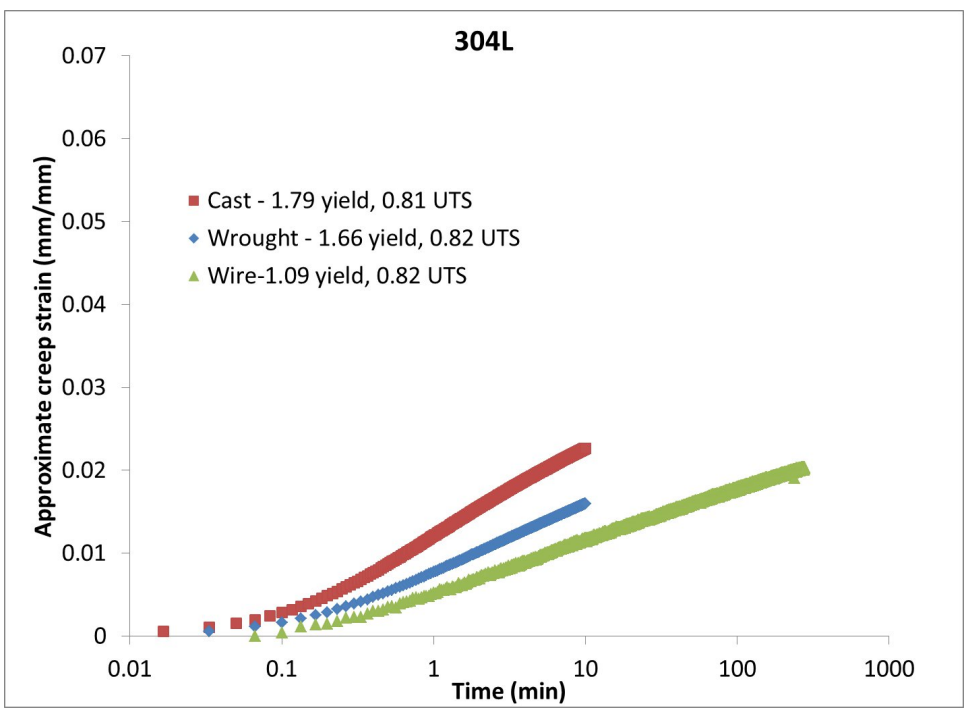

Figure 18. Plots of creep in three different varieties of 304L at approximately 0.82 σ_u

Fitting data from the results section to models from literature

The literature review section of this report references 61 papers on room temperature creep. This section will examine whether the data collected in this report can be modeled by constitutive equations from the literature.

Andrade's equation from his 1910 paper [64] is one of the first equations to be fit to creep of any sort, and in fact he performed some experiments on lead at 15 °C. This equation is purely empirical, since the theory of dislocations did not yet exist. The equation he proposed is:

$$\epsilon = \epsilon_0(1 + \beta t^{\frac{1}{3}})e^{kt} \tag{1}$$

Where ϵ_0 is a term relating to the plastic creep strain, β is related to the non-viscous flow, and k is the viscous flow component. Fitting the Andrade equation to some of the data from the 304L dead-weight experiments produces the fits, coefficients, and χ^2 values plotted in Figure 19. While the fit is quite good for the lower stress experiment, a more phenomenological equation would be preferred.

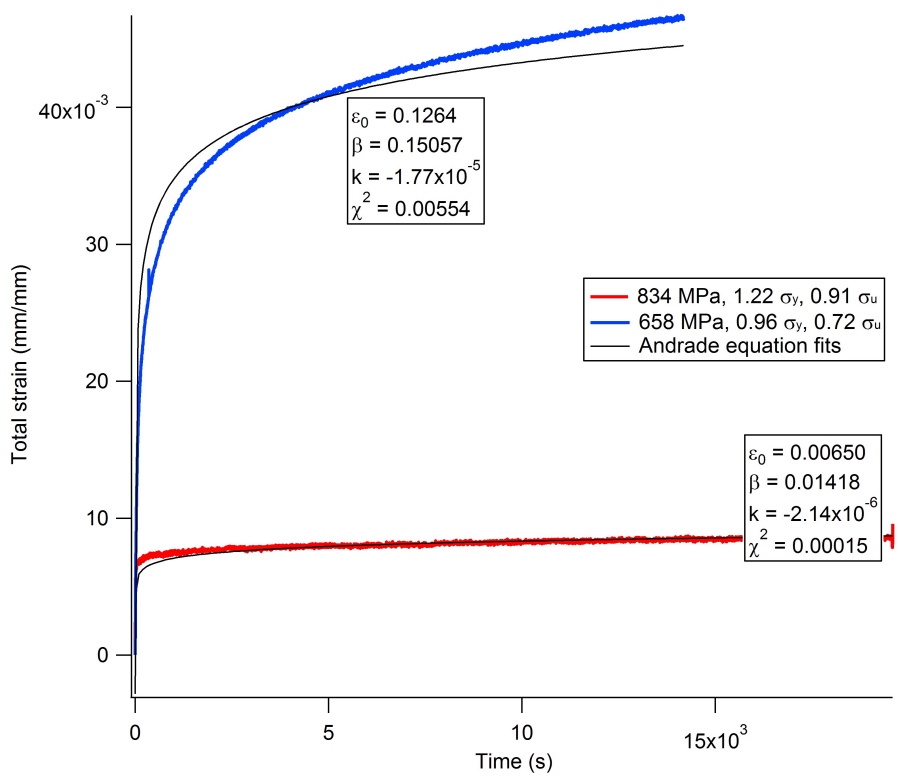

Figure 19. The Andrade equation fit to data from 304L dead-weight creep experiments. Coefficients and χ^2 values for each curve are in the boxes.

While most equations for low temperature creep are based on a logarithmic equation,

low temperature creep data is occasionally represented by a power-law analysis [29]. This analysis assumes that the Holloman flow equation applies.

$$\sigma = K\epsilon^n \dot{\epsilon}^m \tag{2}$$

where K, n, and m are constants. This equation is solved for $\dot{\epsilon}$ and integrated to solve for ϵ under constant stress conditions [29]:

$$\epsilon = \left(\frac{\sigma}{K}\right)^{\frac{1}{m+n}} \left(\frac{m+n}{m}\right)^{\frac{m}{m+n}} t^{\frac{m}{m+n}} \tag{3}$$

This equation uses the creep strain rather than the total strain to fit the equation. Fitting it to the two 304L data curves produces a marginal fit plotted in Figure 20. Like the Andrade equation, the power-law equation is purely empirical.

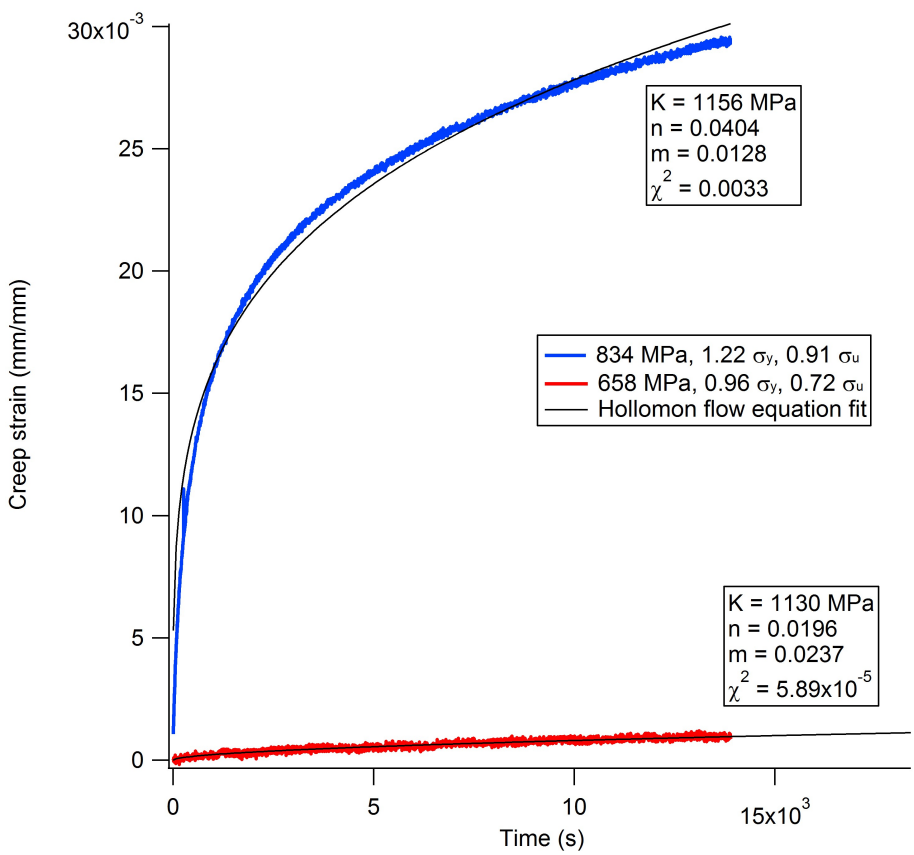

Figure 20. The Hollomon equation as formulated by Neeraj fit to data from 304L dead-weight creep experiments. Coefficients and χ^2 values for each curve are in the boxes.

Mott and Nabarro's equation [22] describes creep which is allowed by dislocations which are able to pass via a quantum tunneling effect through barriers they would not normally thermally be able to overcome . As discussed previously, this theory and the equation which is derived from it have no provision for generation of dislocations during logarithmic creep.

$$\epsilon = [AkT \ln(\gamma t)]^{2/3} \tag{4}$$

where A and γ are constants. The Mott equation is fit to the 304L dead-weight data and plotted in Figure 21. The Mott equation is a a worse fit than the Andrade equation for the higher stress experiment.

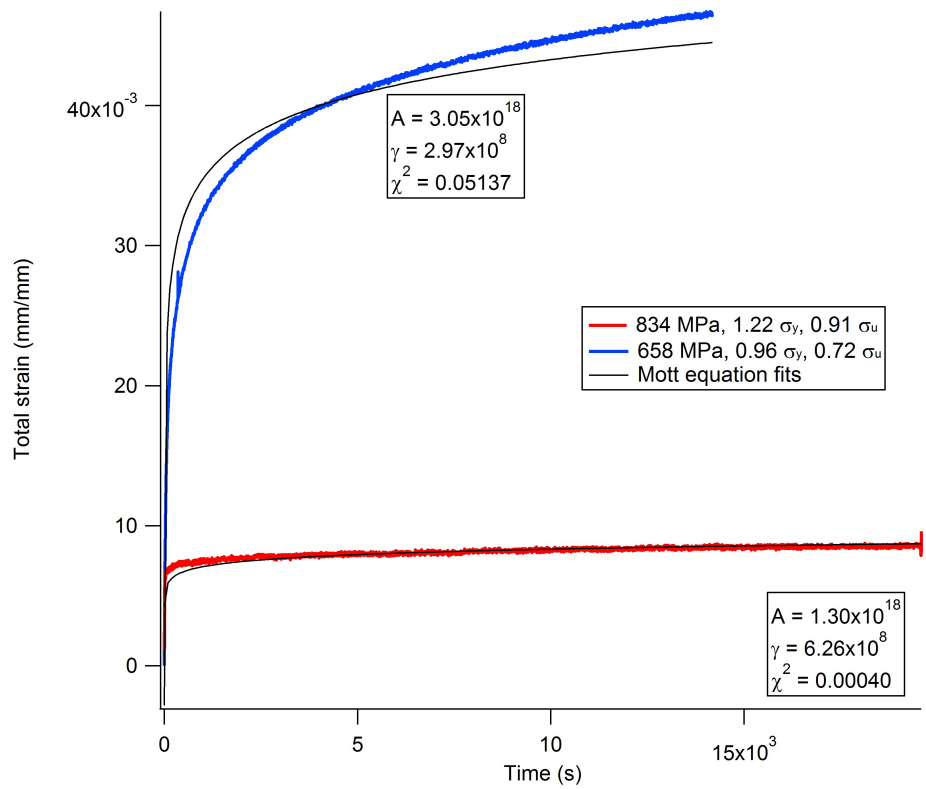

Figure 21. The Mott equation fit to data from 304L dead-weight creep experiments. Coefficients and χ^2 values for each curve are in the boxes.

Further development of the Mott equation with the understanding that dislocation source activation is also important in creep lead to the Mott-Nabarro logarithmic equation [65].

$$\epsilon = \epsilon_0 + \epsilon_1[\ln(t + t_0)]^{2/3} \tag{5}$$

where constants ϵ_0 and t_0 allow the logarithmic portion of the creep curve to be joined

to the instantaneous plastic strain and ϵ_1 is a constant. This equation fits the creep data from 304L dead-weight testing very nicely (Figure 22).

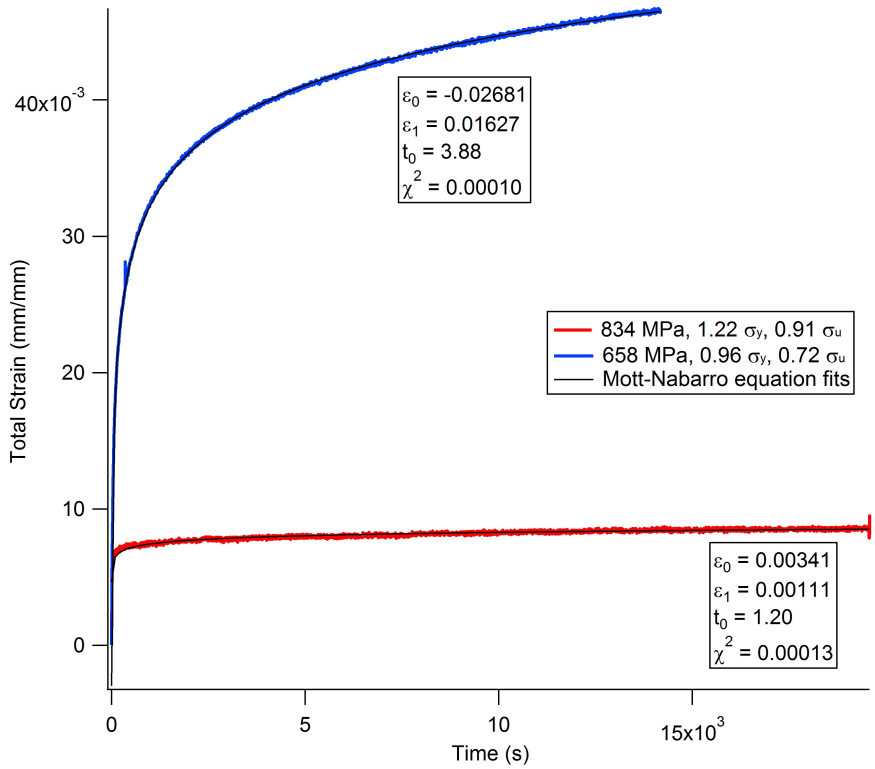

Figure 22. The modified Mott equation fit to data from 304L dead-weight creep experiments. Coefficients and χ^2 values for each curve are in the boxes.

Although the modified Mott equation fits the data well, and is based on reasoning from physical reality, the coefficients in the equations are still difficult to relate to any physically measurable values. An approach suggested by Orowan [66] and further derived in Nabarro's book [65] based on the assumption that creep rate is proportional to the stress, uses coefficients which can actually be related to physical measurements. The logic behind the equation is that after a strain has occurred, the effective stress is reduced by some internal stress which is dependent on the work hardening rate. A similar equation is derived in Kassner's review paper [67], although some different parameters are used.

$$\epsilon = \frac{kT}{Vh}\left\{\ln\left[\frac{Vh\dot{\epsilon}_0(t+t_0)}{kT}\right] - \frac{U_0 - V\sigma}{kT}\right\} \tag{6}$$

where k is Boltzmann's constant, T is temperature in Kelvin, V is activation volume, h is the coefficient of work hardening, $\dot{\epsilon}_0$ is a constant related to the initial plastic strain rate, U_0 is an activation energy constant, σ is the applied stress, and

$$t_0 = \frac{kT}{Vh\dot{\epsilon}_0} e^{\left(\frac{U_0 - V\sigma}{kT}\right)} \tag{7}$$

One advantage of this equation over the others which have been presented is that it includes a stress term. In our experiments, the main parameter that was changed and which affected the resulting strain was the stress, so an equation which contains a stress dependence seems like a logical choice. The activation volume, V, is often considered to be product of the obstacle spacing, l, the Burger's vector, b, and the width of the obstacle, d. More dislocations will be generated at higher stresses, which decreases l, therefore decreasing V. The work hardening coefficient, h, is known to decrease with increasing stress as the work hardening rate decreases [68]. The initial plastic strain rate should increase with increasing stress. It makes intuitive sense that when more stress is applied, the speed at which the material changes shape should increase. This is also supported by the general equation which relates the strain rate to the applied stress [68]

$$\dot{\epsilon} = bAN\nu_0 e^{\left(-\frac{U(\tau)}{kT}\right)} \tag{8}$$

where b is the Burger's vector length, A is the area of the slip plane, ν_0 is a frequency factor determined by the nature of the obstacles, and $U(\tau)$ is the activation energy which depends on the applied shear stress.

While the activation energy, U depends on the applied shear stress, the activation energy constant U_0 from Equation 6 is constant with stress. The parameters are related as follows:

$$U = U_0 - V(\sigma - h\epsilon) \tag{9}$$

Based on the above arguments, V, h, and $\dot{\epsilon}_0$ were allowed to vary with varying applied stress when fitting Equation 6 to data, while U_0 was fixed. T and σ were known values from the experiment. Figure 23 shows the results of fitting Equation 6 to several 304L dead-weight curves.

As a check whether this equation makes physical sense, we can compare the values of the coefficients from the fits to the data to what would be expected for the various parameters. For activation volume, V, expected values are in the 2×10^{-29} m^3 range and the activation volume should decrease with increasing stress. For coefficient of work hardening, h, values are in the 1×10^{10} Pa range and it should also decrease with increasing stress. Reported activation energies are in the $10^{-20} - 10^{-22}$ J range. It is difficult to find reported values for the instantaneous plastic strain rate term, $\dot{\epsilon}_0$. The derivation of a similar equation to Equation 6 [67] uses

$$NV\nu_0 \tag{10}$$

where N is number of dislocations per volume and ν_0 is an atomic frequency on the order of the Debye frequency instead of $\dot{\epsilon}_0$. This relationship can be used to estimate an expected

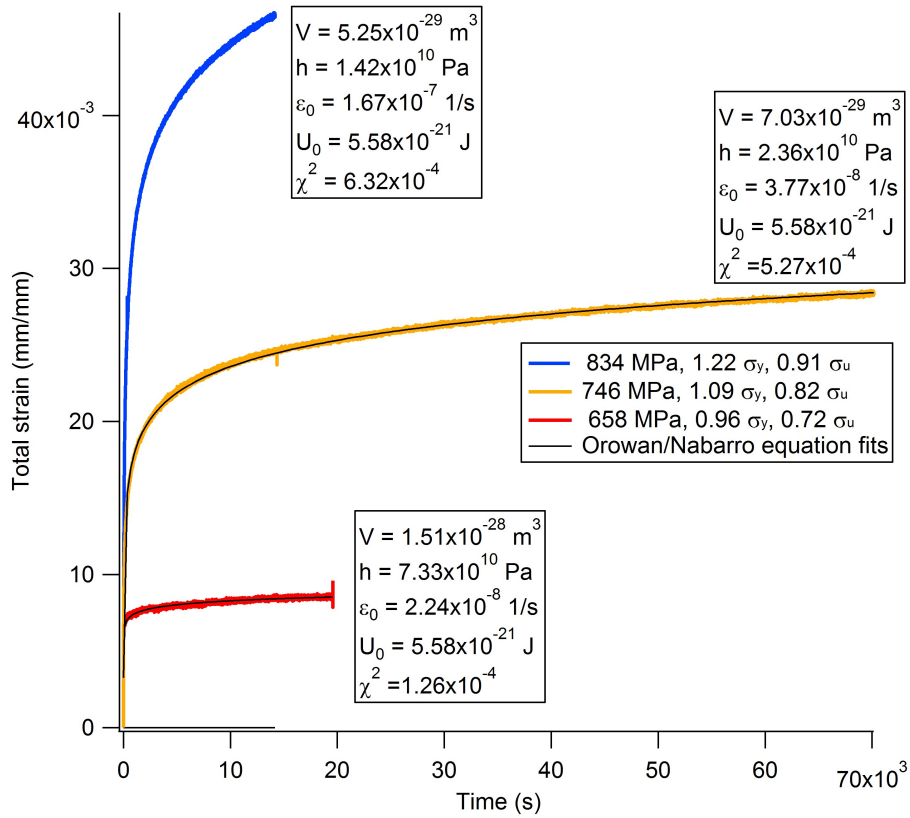

Figure 23. The Orowan/Nabarro equation fit to data from 304L dead-weight creep experiments. Coefficients and χ^2 values for each curve are in the boxes.

value for $\dot{\epsilon}_0$. There are approximately 10^{10} dislocation segments/m^3 in an alloy [65], although the order of magnitude will depend strongly on how much work hardening is present, and the frequency is on the order of the Debye frequency/10: 10^{12} 1/s [65], so an estimate of $\dot{\epsilon}_0$ would put it in the range of 10^{-7} 1/s and it should increase with increasing stress. The values determined by fitting Equation 6 are slightly smaller than this estimation, but they do increase with increasing stress. As displayed in the boxes in Figure 23, all the values and trends except the value of $\dot{\epsilon}_0$ fit within the expected parameters.

The 304L wire dead-load creep data are the most complete data set that has been collected, and Equation 6 has been found to fit the data well. However, enough data was also collected on the pure Cu wire to attempt to fit the Orowan/Nabarro equation. The results are plotted in Figure 24. At the lowest stress, the equation fits very well, but the behavior begins to deviate from the model at the intermediate stress and is quite poorly described by the model at the highest stress. The coefficients continue to follow the correct trends as described above, although the values for V and and ϵ_0 are outside of their expected ranges for the sample tested at 248 MPa. It is not surprising that the model does not fit well at

the highest stress data because at that stress level the creep is clearly accelerating and the sample failed at the end of the curve. At that point in a creep curve damage is beginning to accumulate in the sample which is not described by the model. However, the deviation from the model a intermediate stress is curious. It may indicate that creep damage is already accumulating, or it could indicate that the mechanism of creep in pure copper is not well described by the relationship described in Equation 6 between the applied stress and the strain-hardening internal stress. Matsunaga [41] theorized that because of copper's low stacking fault energy, the creep proceeds through dislocation glide because cross-slip is less favorable. 304L has an even lower stacking fault energy (17 mJ/m^2 [69]) than copper (41 mJ/m^2 [70]), so according to that argument, both should proceed by dislocation glide rather than cross-slip.

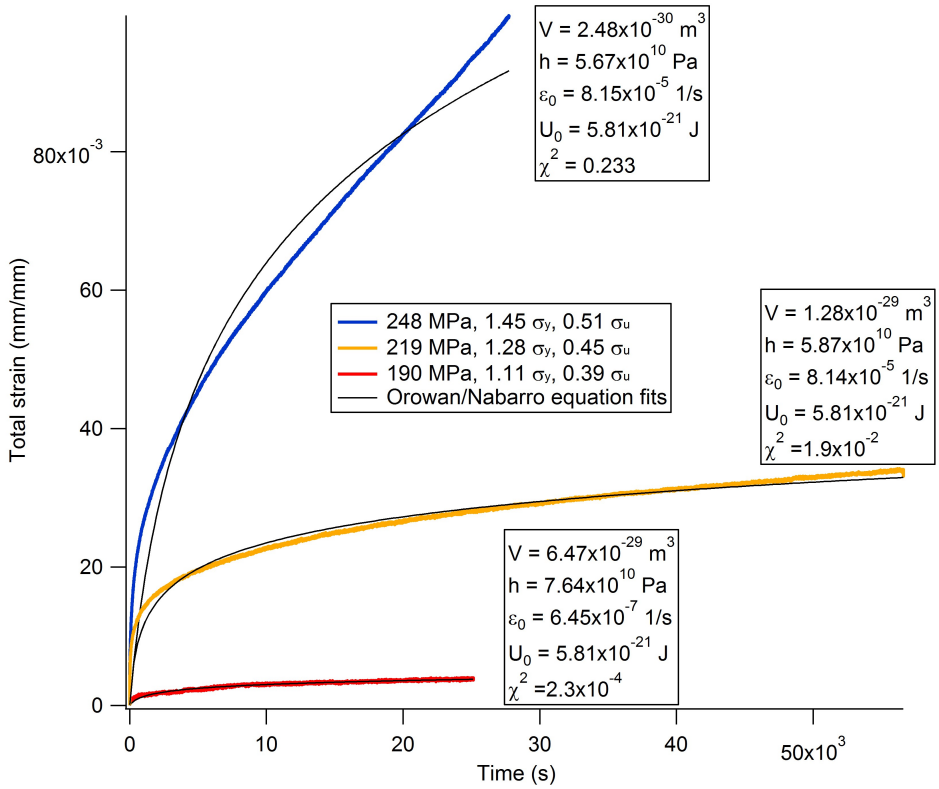

Figure 24. The Orowan/Nabarro equation fit to data from pure Cu dead-weight creep experiments. Coefficients and χ^2 values for each curve are in the boxes.

Dislocation generation vs. dislocation exhaustion

The major division amongst the literature papers reviewed is whether or not they considered the generation of dislocations during creep or stress relaxation. There are are more papers which include dislocation generation as a mechanism than there are that describe

creep as some variety of an exhaustion process, and the data supporting dislocation generation is convincing. It is difficult to conceive of an alternate explanation which does not include dislocation generation for some of the more complicated behavior described, for example in Savage [44], Thompson and Odegard [43], and Kremple [17, 47]. As further support for theories including dislocation generation, the two equations which include dislocation generation (Modified Mott, Equation 22 and Orowan-Nabarro, Equation 6) fit the 304L data the best of all the literature equations plotted. In fact, the way the parameters of the Orowan-Nabarro equation, in particular V, decreases with increasing stress when the equations are fit to data reinforces the theory that dislocation generation is occurring. TEM analysis could be performed to provide more experimental proof for generation of dislocations during creep.

Conclusion

The data collected in this study along with the literature data reviewed provide convincing evidence that room temperature creep and stress relaxation do occur across many metal alloys. Long-term experiments on 304L wires exhibited creep strains approaching 5% for samples loaded near the quasi-static tensile yield stress, which could be a significant strain in some applications.

The literature and data reviewed supports the theory that dislocations are generated via some mechanism during low temperature creep. Many equations have been proposed to describe low temperature creep, but Orowan's equation (Equation 6) fits well, contains constants which have physical meaning, includes an applied stress term, and allows for the generation of dislocations during creep.

Further work with higher resolution strain measurement is needed to determine whether creep saturates after a period of time. Additionally, more detailed experiments on other alloys besides 304L would be helpful to better understand the effects of crystal structure and microstructure on room temperature creep. Not all components are loaded in tension at a constant stress, which is the relevant stress state for the present creep experiments. Stress relaxation is more relevant to many applications, for example in springs. Although creep and stress relaxation are similar in that they are time-dependent phenomena, there is not much information about how they relate to each other, so stress relaxation experiments should also be performed.

References

[1] M. Kassner, *Fundamentals of Creep in Metals and Alloys.* Elsevier, 2009.

[2] J. R. Ellis, D. N. Robinson, and C. E. Pugh, "Behavior of annealed type 316 stainless steel under monotonic and cyclic biaxial loading at room temperature," *Nuclear Engineering and Design*, vol. 47, no. 1, pp. 115–123, 1978.

[3] D. Pilo, W. Reik, P. Mayr, and E. Macherauch, "Cyclic induced creep of a plain carbon steel at room temperature," *Fatigue of Engineering Materials and Structures*, vol. 1, pp. 287–295, 1979.

[4] C. Liu, P. Liu, Z. B. Zhao, and D. O. Northwood, "Room temperature creep of a high strength steel," *Materials and Design*, vol. 22, no. 4, pp. 325–328, 2001.

[5] C. Liu, Bhole, and D. Northwood, "The effects of ferrite content and morphology on the mechanical properties and room temperature creep of quenched and tempered SAE 4340 steel," *JSME International Journal*, vol. 46, no. 3, 2003.

[6] M. E. Kassner, R. S. Rosen, and G. A. Henshall, "Delayed mechanical failure of silver-interlayer diffusion bonds," *Metallurgical Transactions A*, vol. 21, no. 12, pp. 3085–3100, 1990.

[7] C. Krapf, *Stress relaxation of post-tensioned stainless steel rods for bridge pier cap shear strengthening.* PhD thesis, 2010.

[8] T. Yamada, K. Kawabata, E. Sato, K. Kuribayashi, and I. Jimbo, "Presences of primary creep in various phase metals and alloys at ambient temperature," *Materials Science and Engineering A*, vol. 387-389, pp. 719–722, 2004.

[9] E. Sato, T. Yamada, H. Tanaka, and I. Jimbo, "Categorization of ambient-temperature creep behavior of metals and alloys on their crystallographic structures," *Materials Transactions*, vol. 47, no. 4, pp. 1121–1126, 2006.

[10] H. Tanaka, T. Yamada, E. Sato, and I. Jimbo, "Distinguishing the ambient-temperature creep region in a deformation mechanism map of annealed CP-Ti," *Scripta Materialia*, vol. 54, no. 1, pp. 121–124, 2006.

[11] Z. Jie, M. Tao, and N. Defu, "The occurrence of room-temperature creep in cracked 304 stainless steel specimens and its effect on crack growth behavior," *Materials Science and Engineering: A*, vol. 483-484, pp. 572–575, 2008.

[12] M. A. Imam and C. M. Gilmore, "Room temperature creep of Ti-6AI-4V," *Metallurgical Transactions A*, vol. 10, no. 4, pp. 419–425, 1979.

[13] B. Odegard and A. Thompson, "Low temperature creep of Ti-6 Al-4 V," *Metallurgical Transactions*, vol. 5, no. 5, pp. 1207–1213, 1974.

[14] W. Reimann, "Room temperature creep in Ti-6Al-4V," *Journal of Materials*, vol. 6, no. 4, pp. 926–940.

[15] T. Matsunaga, T. Kameyama, K. Takahashi, and E. Sato, "Constitutive relation for ambient-temperature creep in hexagonal close-packed metals," *Materials Transactions*, vol. 50, no. 12, pp. 2858–2864, 2009.

[16] H. Luthy, A. K. Miller, and O. D. Sherby, "The stress and temperature dependence of steady-state flow at intermediate temperatures for pure polycrystalline aluminum," *Acta Metallurgica*, vol. 28, no. 2, pp. 169–178, 1980.

[17] E. Krempl, "An experimental study of room-termpetaure rate-sensitivity, creep, and relaxation of AISI type 304 stainless steel," *Journal of Mechanics and Physics of Solids*, vol. 27, pp. 363–375, 1979.

[18] A. Oehlert and A. Atrans, "Overview No. 114 room temperature creep of high strength steels," *Acta Metallurgica Materialia*, vol. 42, no. 5, pp. 1493–1508, 1994.

[19] T. Langdon and F. Mohamed, "A simple method of constructing an Ashby-type deformation mechanism map," *Journal of Materials Science*, vol. 13, no. 6, pp. 1282–1290, 1978.

[20] G. Gao and S. Dexter, "Effect of hydrogen on creep behavior of Ti-6AI-4V alloy at room temperature," *Metallurgical and Materials Transactions A*, vol. 18, no. 13, pp. 1125–1130, 1987.

[21] U. Kivisakk, "Relation of room temperature creep and microhardness to microstructure and HISC," *Materials Science and Engineering A*, vol. 527, pp. 7684–7688, 2010.

[22] N. Mott and F. Nabarro, "Report of a conference on the strength of solids," 1948.

[23] N. Mott, "LVII. creep in metal crystals at very low temperatures," *Philosophical Magazine*, vol. 1, no. 6, pp. 568–572, 1956.

[24] I. Gupta and J. Li, "Stress relaxation, internal stress, and work hardening in some BCC metals and alloys," *Metallurgical and Materials Transactions B*, vol. 1, no. 8, pp. 2323–2330, 1970.

[25] C. Barklay, J. Howe, and D. Kramer, "Investigation of stress rupture tested neutron irradiated tantalum alloys," in *Space Technology and Applications Internation Forum 2008*, vol. 969, pp. 439–445, American Institute of Physics.

[26] A. Brahmi, T. Gerique, M. Lieblich, and M. Torralba, "Creep behavior of a rapidly solidified Al-5Cr-2Zr alloy between room temperature and 823K," *Scripta Materialia*, vol. 35, no. 12, pp. 1449–1454, 1996.

[27] S. Suri, G. B. Viswanathan, T. Neeraj, D. H. Hou, and M. J. Mills, "Room temperature deformation and mechanisms of slip transmission in oriented single-colony crystals of an α/β titanium alloy," *Acta Materialia*, vol. 47, no. 3, pp. 1019–1034, 1999.

[28] W. H. Miller, R. T. Chen, and E. A. Starke, "Microstructure, creep, and tensile deformation in Ti-6Al-2Nb-1Ta-0.8Mo," *Metallurgical Transactions A*, vol. 18, no. 8, pp. 1451–1468, 1987.

[29] T. Neeraj, D. Hou, G. Daehn, and M. Mills, "Phenomenological and microstructureal analysis of room temperature creep in titanium alloys," *Acta Materialia*, vol. 48, pp. 1225–1238, 2000.

[30] S. H. Wang and W. X. Chen, "Room temperature creep deformation and its effect on yielding behaviour of a line pipe steel with discontinuous yielding," *Materials Science and Engineering A*, vol. 301, no. 2, pp. 147–153, 2001.

[31] Z. Zhao, D. Northwood, C. Liu, and Y. Liu, "A new method for improving the resistance of high strength steel wires to room temperature creep and low cycle fatigue," *Journal of Materials Processing Technology*, vol. 89-90, pp. 569–573, 1999.

[32] C. Liu, Z. Zhao, and D. O. Northwood, *Effect of heat treatments on room temperature creep strain of a high strength steel*, vol. 171-1 of *Key Engineering Materials*, pp. 403–409. Zurich-Uetikon: Transtec Publications Ltd, 2000.

[33] R. W. Rohde and T. V. Nordstrom, "On stress relaxation experiments," *Scripta Metallurgica*, vol. 7, no. 3, pp. 317–322, 1973.

[34] M. A. Fortes and J. G. Proena, "Comments on on stress relaxation experiments," *Scripta Metallurgica*, vol. 7, no. 11, pp. 1149–1152, 1973.

[35] R. W. Rohde and T. V. Nordstrom, "Reply to comments on, on stress relaxation experiments," *Scripta Metallurgica*, vol. 7, no. 11, pp. 1227–1228, 1973.

[36] J. C. M. Li, "A dislocation mechansim of transient creep," *Acta Metallurgica*, vol. 11, no. 11, pp. 1269–1270, 1963.

[37] J. Shen, K.-i. Ikeda, S. Hata, and H. Nakashima, "Transient creep in high-purity aluminum at ultra-low strain rate and room temperature by constant stress and changing-stress experiments," *Materials Transactions*, vol. 52, no. 10, pp. 1885–1889, 2011.

[38] W. Schmidt and H. Dietrich, "Connection between room-temperature-creep and behavior of stress-strain-curve of metallic materials," *Zeitschrift Fur Metallkunde*, vol. 63, no. 10, p. 654, 1972.

[39] W. K. Miller, "Creep of die cast AZ91 magnesium at room-temperature and low stress," *Metallurgical Transactions A*, vol. 22, no. 4, pp. 873–877, 1991.

[40] T. Schober and H. Trinkaus, "Room-temperature creep of tantalum tritides," *Journal of Applied Physics*, vol. 67, no. 12, pp. 7587–7590, 1990.

[41] T. Matsunaga, S. Ueda, and E. Sato, "New creep region in pure face-centered cubic metals at low temperatures," *Scripta Materialia*, vol. 63, no. 5, pp. 516–519, 2010.

[42] R. Zeyfang, R. Martin, and H. Conrad, "Low temperature creep of titanium," *Materials Science and Engineering*, vol. 8, no. 3, pp. 134–140, 1971.

[43] A. Thompson and B. Odegard, "The influence of microstructure on low temperature creep of Ti-5 Al-2.5 Sn," *Metallurgical Transactions*, vol. 4, no. 4, pp. 899–908, 1973.

[44] M. Savage, T. Neeraj, and M. Mills, "Observations of room-temperature creep recovery in titanium alloys," *Metallurgical and Materials Transactions*, vol. 33A, pp. 891–898, 2002.

[45] P. Oberson and S. Ankem, "The effect of time-dependent twinning on low temperature (<0.25*T_m) creep of an alpha-titanium alloy," *International Journal of Plasticity*, vol. 25, pp. 881–900, 2009.

[46] R. W. Armstrong and P. Worthington, *A constitutive relation for deformation twinning in body centered cubic metals*, pp. 401–414. New York: Plenum Press, 1973.

[47] D. Kujawski, V. Kallianpur, and E. Krempl, "An experimental-study of uniaxial creep, cyclic creep and relaxation of AISI type-304 stainless-steel at room-temperature," *Journal of the Mechanics and Physics of Solids*, vol. 28, no. 2, pp. 129–148, 1980.

[48] D. Kujawski and E. Krempl, "The rate (time)-dependent behavior of Ti-7Al-2Cb-1Ta titanium alloy at room temperature under quasi-static monotonic and cyclic loading," *Journal of Applied Mechanics*, vol. 48, pp. 55–63, 1981.

[49] R. W. Armstrong and S. M. Walley, "High strain rate properties of metals and alloys," *International Materials Reviews*, vol. 53, no. 3, pp. 105–128, 2008.

[50] T. Alden, "Theory of mobile dislocation density: Application to the deformation of 304 stainless steel," *Metallurgical Transactions A*, vol. 18, no. 1, pp. 51–62, 1987.

[51] T. H. Alden, "Theory of plastic and viscous deformation," *Metallurgical Transactions A*, vol. 18, no. 6, pp. 811–826, 1987.

[52] G. A. Henshall and A. K. Miller, "Simplifications and improvements in unified constitutive equations for creep and plasticity - I. Equations development," *Acta Metallurgica et Materialia*, vol. 38, no. 11, pp. 2101–2115, 1990.

[53] G. A. Henshall and A. K. Miller, "Simplifications and improvements in unified constitutive equations for creep and plasticity - II. Behavior and capabilities of the model," *Acta Metallurgica et Materialia*, vol. 38, no. 11, pp. 2117–2128, 1990.

[54] B. L. Boyce, T. B. Crenshaw, and M. F. Dilmore, "The strain-rate sensitivity of high-strength high-toughness steels," tech. rep., Sandia National Laboratories, 2006. SAND2007-0036.

[55] J. Lichtenfeld, C. Tyne, and M. Mataya, "Effect of strain rate on stress-strain behavior of alloy 309 and 304L austenitic stainless steel," *Metallurgical and Materials Transactions A*, vol. 37, no. 1, pp. 147–161, 2006.

[56] R. W. Neu and H. Sehitoglu, "Low-temperature creep of a carburized steel," *Metallurgical Transactions A*, vol. 23, no. 9, pp. 2619–2624, 1992.

[57] M. Tendo, T. Takeshita, and T. Nakazawa, "Effects of solute carbon and nitrogen on room-temperature creep of austenitic stainless-steels," *Journal of the Japan Institute of Metals*, vol. 59, no. 6, pp. 620–626, 1995.

[58] Z. A. Yang, Z. G. Wang, and S. Q. Wang, "Effect of grain-size on cyclic creep-behavior in a commercially pure aluminum at room-temperature," *Materials Science and Engineering A*, vol. 102, no. 1, pp. 17–23, 1988.

[59] K. Ishikawa, H. Okuda, and Y. Kobayashi, "Creep behaviors of highly pure aluminum at lower temperatures," *Materials Science and Engineering: A*, vol. 234236, no. 0, pp. 154–156, 1997.

[60] K. Ishikawa, M. Maehara, and Y. Kobayashi, "Mechanical modeling and microstructural observation of pure aluminum crept under constant stress," *Materials Science and Engineering: A*, vol. 322, no. 12, pp. 153–158, 2002.

[61] J. T. Evans and R. N. Parkins, "Creep induced by load cycling in a C-Mn steel," *Acta Metallurgica*, vol. 24, no. 6, pp. 511–515, 1976.

[62] P. S. G. Bennett and J. T. Evans, "Creep stimulated by interrupted loading in copper and copper-1% cadmium," *Materials Science and Engineering*, vol. 38, no. 2, pp. 111–122, 1979.

[63] S. H. Wang and W. X. Chen, "A study on the pre-cyclic-load-induced burst of creep deformation of a pipeline steel under subsequent static load," *Materials Science and Engineering A*, vol. 325, no. 1-2, pp. 144–151, 2002.

[64] E. d. C. Andrade, "On the viscous flow in metals, and allied phenomena," *Proceedings of the Royal Society A*, vol. 84, p. 1, 1910.

[65] F. Nabarro and F. De Villiers, *Physics of Creep.* CRC Press, 1995.

[66] E. Orowan *Z Physik*, vol. 89, p. 614, 1934.

[67] M. E. Kassner and K. Smith, "Low temperature creep plasticity," *Journal of Materials Research and Technology*, vol. 3, no. 3, pp. 280–288, 2014.

[68] R. W. K. Honeycombe, *The Plastic Deformation of Metals.* Edward Arnold Publishers LTD, 1968.

[69] R. Schramm and R. Reed, "Stacking fault energies of seven commercial austenitic stainless steels," *Metallurgical Transactions A*, vol. 6A, pp. 1345–51, 1975.

[70] P. S. Branicio, J. Y. Zhang, and D. J. Srolovitz, "Effect of strain on the stacking fault energy of copper: A first-principles study," *Physical Review B*, vol. 88, no. 6, p. 064104, 2013.

DISTRIBUTION:

1	MS 0888	Regan Stinnett, 1836
1	MS 0889	Brad Boyce, 1831
1	MS 0889	Joe Puskar, 1831
1	MS 0889	Tom Crenshaw, 1831
1	MS 9902	Bob Chambers, 1526
1	MS 0899	Technical Library, 9536 (electronic copy)

Sandia National Laboratories